Carlos André Mendonça Gomes

Licenciatura em Ciências da Engenharia Química e Bioquímica

Study of multi-component systems in polybenzimidazole membrane formation and their impact on membrane performance

Dissertação para obtenção do Grau de Mestre em
Engenharia Química e Bioquímica

Orientador: Professor Andrew Livingston, Imperial College London

Co-orientadores: Professora Isabel Coelhoso, Universidade Nova de Lisboa

Júri:

Presidente: Ana Maria Martelo Ramos

Arguente: Svetlozar Gueorguiev Velizarov

Vogal: Isabel Maria Rola Coelhoso

FACULDADE DE CIÊNCIAS E TECNOLOGIA
UNIVERSIDADE NOVA DE LISBOA

Outubro, 2013

Carlos André Mendonça Gomes
Licenciatura em Ciências da Engenharia Química e Bioquímica

STUDY OF MULTI-COMPONENT SYSTEMS IN POLYBENZIMIDAZOLE MEMBRANE FORMATION AND THEIR IMPACT ON MEMBRANE PERFORMANCE

Dissertação para obtenção do Grau de Mestre em
Engenharia Química e Bioquímica

Orientador: Professor Andrew G. Livingston (Imperial College London)

Co-orientador: Professora Isabel Coelhoso (Universidade Nova de Lisboa)

IMPERIAL COLLEGE LONDON
Faculty of Engineering
Department of Chemical Engineering and Chemical Technology

UNIVERSIDADE NOVA DE LISBOA
Faculdade de Ciências e Tecnologia
Departamento de Química

Outubro 2013

Study of multi-component systems in polybenzimidazole membrane formation and their impact on membrane performance

ACKNOWLEDGMENT

First of all, I would like to thank Professor Andrew Livingston for having me in his research group.

I am deeply grateful to Irina Valtcheva, my daily supervisor, who helped me through the whole project, including writing this thesis.

I would like to thank all the other members of the Separation Engineering and Technology research group for their support during my stay at Imperial College London.

I would like also to thank Professor Isabel Coelhoso for being always available to help with any questions and showing interest in my work.

Last but not least, I would like to thank my family and friends for their emotional help, encouragement and understanding.

ABSTRACT

Integrally skinned asymmetric polybenzimidazole (PBI) membranes suitable for organic solvent nanofiltration (OSN) were prepared via phase inversion and several changes were implemented in the dope solutions in order to control their molecular weight cut-off (MWCO). Initially, uncrosslinked membranes with different polymer concentrations were tested to investigate their impact on membrane performance. On a second approach, several co-solvents were added in the dope solutions of PBI membranes. Coupling this methodology with chemical crosslinking, using an aromatic bi-functional crosslinker, provided solvent stable membranes with several MWCOs in the nanofiltration range and high permeance. Further variation of membrane dope parameters was tested in order to study membrane formation impact on membrane performance. Total solubility parameters of the chosen co-solvents were calculated, and a correlation between this tool and membrane performance was studied. Even though it was not possible to withdraw conclusions on a fundamental level, from the correlation of the total solubility parameters with membrane performance, this work demonstrates the possibility of developing PBI OSN membranes using different co-solvents and opens up future possibilities for controlling the MWCO of these membranes. A post-treatment study was also conducted in order to examine its impact in membrane performance.

Keywords: Organic Solvent Nanofiltration (OSN), Polibenzamidazole (PBI), Membrane formation, Controlling molecular weight cut-off (MWCO)

RESUMO

Diversas membranas resistentes a solventes orgânicos (OSN) foram preparadas com Polybenzimidazole (PBI) via *phase inversion* e várias alterações foram implementadas nas soluções de modo a controlar o peso molecular que rejeitam (MWCO). Inicialmente, membranas sem *crosslink* foram preparadas com diferentes concentrações de polímero e foram testadas de modo a investigar o seu impacto na performance das membranas. Numa segunda abordagem, diversos co-solventes foram adicionados às soluções de PBI. A conjugação da adição de co-solventes com *crosslinking* com um *crosslinker* aromático bi-funcional deu origem a membranas estáveis com vários MWCO na região da nanofiltração com elevada permeabilidade. Outros parâmetros foram estudados de modo a verificar o impacto da formação da membrana na sua performance. Parâmetros de solubilidade dos co-solventes foram calculados e estudou-se uma correlação entre estes e a performance das membranas. Ainda que não tenha sido possível tirar conclusões a um nível fundamental, este trabalho demonstra a possibilidade de desenvolver membranas com PBI para OSN com diferentes co-solventes de modo a obter diferentes MWCO. Um estudo de pos-tratamento também foi desenvolvido de modo a examinar o seu impacto na performance das membranas

Palavras-chave: Nanofiltração em solventes orgânicos (OSN), Polibenzamidazole (PBI), Formação de membranas, Controlar molecular weight cut-off (MWCO)

TABLE OF CONTENTS

LIST OF FIGURES

LIST OF TABLES

LIST OF ABBREVIATIONS

DBX	α,α'-dibromo-p-xylene
DMAc	N,N-dimethylacetamide
DMF	N,N-dimethylformamide
DMSO	dimethylsulfoxide
DXN	1,4-dioxane
EtOH	ethanol
FT-IR	Fourier transform – infrared spectroscopy
HPLC	High Pressure Liquid Chromatography
IPA	propan-2-ol
IS	integrally skinned
MeCN	acetonitrile
MeOH	methanol
MF	microfiltration
MWCO	molecular weight cut-off
NF	nanofiltration
NMP	methylpyrrolidinone
OSN	organic solvent nanofiltration
PAN	polyacrylonitrile
PBI	polybenzimidazole
PEEK	polyetheretherkethone
PEG	polyethylene glycol
PI	polyimide
PP	polypropylene
PS	polystyrene
RO	reverse osmosis
SEM	scanning electron microscopy
SRNF	solvent resistant nanofiltration

TFC	thin film composite
THF	tetrathydrofuran
UF	ultrafiltration

NOMENCLATURE

μ	Viscosity (cP)
A	Membrane area (m^2)
B	Solvent permeance ($L.m^{-2}.h^{-1}.bar^{-1}$)
C	Concentration ($g.L^{-1}$)
$c_{i,F}$	Concentration of solute in the feed ($g.L^{-1}$)
$c_{i,P}$	Concentration of solute in the permeate ($g.L^{-1}$)
D	Diffusivity coefficient ($m^2.s^{-1}$)
E_{coh}	Cohesion energy ($J.mol^{-1}$)
J	Flux ($L.m^{-2}.h^{-1}$)
MW	Molecular weight ($g.mol^{-1}$)
P	Pressure (bar)
R	Rejection of solute (%)
T	Temperature (T)
t	Time (h)
V	Volume (L)
V_i	Mole volume
X_i	Mole fraction
Δ	Gradient
δ	Solubility parameter (MPa.s)
φ	Association parameter

1. Literature Review

1.1. Membrane technology

1.1.1. Membranes: Definition and classification

Membrane technology is interdisciplinary, involving chemists to develop new membrane materials; mathematicians to describe the transport properties of different membranes using mathematical models to predict their separation characteristics; and chemical engineers to design separation processes for large scale industrial utilization. However, the most important element in a membrane process is the membrane itself (Porter, 1990).

A complete definition of a membrane that covers all its aspects is rather difficult. In general, a membrane is a thin, film-like structure that acts as a selective barrier, separating two fluids (gas or liquid), allowing some solutes and solvents to pass through, but not others, when exposed to the action of a driving force (concentration, pressure, temperature gradient, electrical potential) (Figure 1.1). Some components are allowed passage by the membrane into a permeate stream, whereas others are retained by it and accumulate in the retentate stream. Thus, the membrane remains impermeable to specific particles, molecules or substances (Vandezande, Gevers & Vankelecom, 2008).

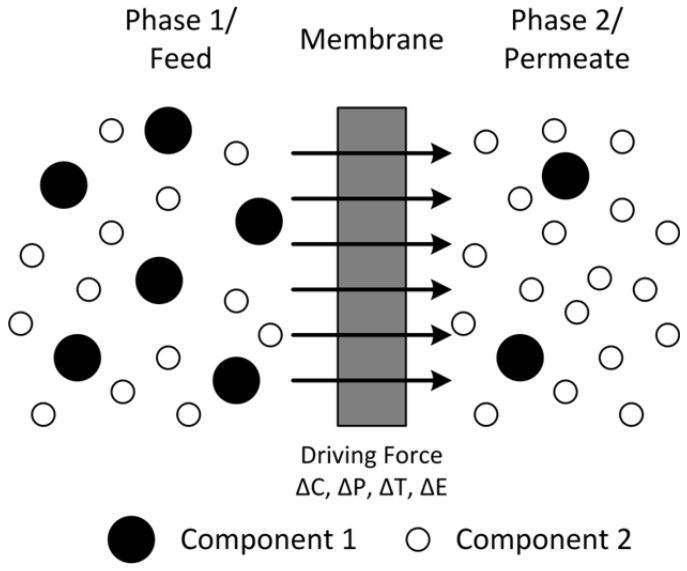

Figure 1.1 – Schematic representation of a membrane system selectively retaining Component 1 and allowing Component 2 to pass through under an applied driving force (Mulder, 1996)

1.1.2. Types of membranes

Membranes can be classified according to their nature and pore size.

- Nature (Mulder, 1996):
    - Synthetic
    - Biological
- Pore Size (IUPAC) (Baker, 2004):
    - RO (Reverse Osmosis) – dense (non-porous)
    - NF (Nanofiltration) – pores smaller than 2 nm
    - UF (Ultrafiltration) – pores from 2 nm to 0.1 μm
    - MF (Microfiltration) – pores from 0.1 μm to 10 μm
    - Conventional filtration – pores from 10 μm to 100 μm

The material selection for synthetic membranes can be based on the membrane film forming properties, chemical and thermal stability, commercial availability and price (Table 1.1).

Synthetic membranes can be divided into ceramic (inorganic) and polymeric (organic).

Ceramic membranes. Ceramic (inorganic) membranes are classified as dense or porous according to their morphology. The most commonly used inorganic membranes are composites consisting of two or more layers. These layers can have different porosity and can be made of different inorganic materials such as Al_2O_3, TiO_2, ZrO_2 or SiO_2 (Baker, 2004).

Different techniques exist for fabricating ceramic membranes such as slip casting, dip-coating, sol-gel and others. Usually they include multiple steps where each step involves a high temperature sintering treatment (Baker, 2004).

Polymeric membranes. Polymeric (organic) membranes can be classified in two categories according to their morphology, symmetric or asymmetric (Figure 1.2). Symmetric membranes are homogeneous and can be nonporous/dense or porous while asymmetric membranes are heterogeneous and can be classified as integrally skinned (IS) or thin film composites (TFCs) (Baker, 2004).

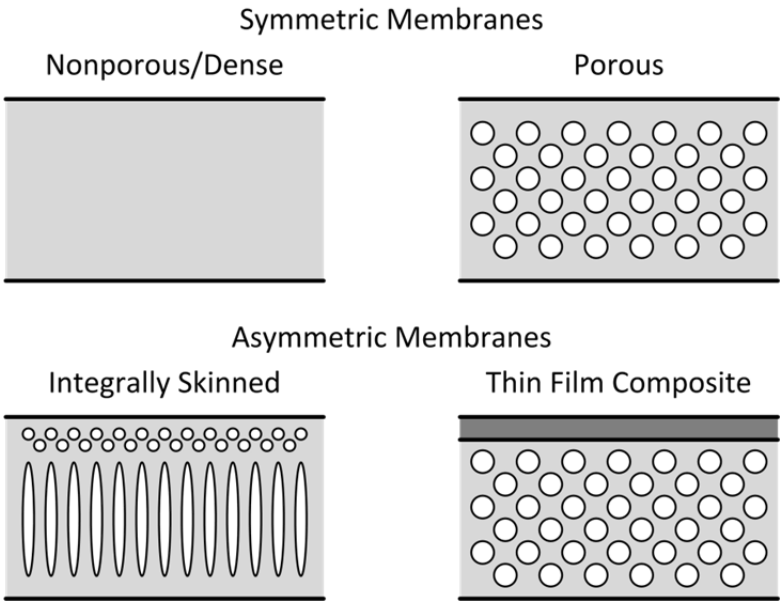

Figure 1.2 – Schematic representation of the four basic polymer membrane types (Baker, 2004)

a) Nonporous/dense membranes. The transport of molecules through dense membranes is a diffusion based process in which the driving force can be a pressure, concentration or electrical potential gradient across the membrane. The phase separation occurs due to a difference in diffusivity and solubility of the solutes in the membrane. This type of membrane is commonly used in gas separation, reverse osmosis and pervaporation. The disadvantage of dense membranes is the high resistance to flow resulting in low flow rates and therefore low feasibility for commercial applications (Baker, 2004).

b) Porous membranes. These membranes consist of a rigid structure with interconnected pores evenly distributed over the membrane. The separation occurs mainly due to size exclusion, which means that only molecules with significant size difference will be separated. Symmetric porous membranes are suitable for ultra- and microfiltration (Baker, 2004).

c) Integrally skinned (IS) membranes. Characteristic for integrally skinned membranes is the non-uniform pore size distribution across the membrane thickness. They consist of a highly porous bottom layer and a less porous top layer, both prepared in one step using the same polymer material. The porous substructure provides mechanical support and prevents the membrane from breaking, whereas the less porous skin layer is responsible for molecular discrimination and flow resistance. Such membranes are usually prepared via phase inversion technique in one step. They are applied in ultra- and nanofiltration as well in gas separation and reverse osmosis (Baker, 2004; Mulder, 1996).

d) Thin film composite (TFC) membranes. TFC membranes consist of two layers (skin and support layer) and are similar to integrally skinned asymmetric membranes. The major difference is that the two layers are made in different steps and have a different chemical composition, which enables the optimisation of the two layers separately. The advantage of using such membranes is the possibility to adapt them to a specific application. The porous support layer is usually an asymmetric UF membrane

prepared via phase inversion while the ultrathin top layer can be obtained through several different techniques – dip coating, spin coating, interfacial polymerisation, plasma deposition and others. TFC membranes are used in reverse osmosis, nanofiltration and gas separation (Drioli & Giorno, 2009; Vandezande, Gevers & Vankelecom, 2008).

Comparison between ceramic and polymeric membranes. In terms of chemical, thermal and structural stability, ceramic membranes perform better than polymeric (Table 1.1). However their production costs, complicated synthesis, handling difficulties and process scale-up are a big obstacle for them to be used more widely (Drioli & Giorno, 2009), therefore polymeric membranes are the ones studied in this dissertation.

Table 1.1 – Comparison between polymeric and ceramic membranes (Drioli & Giorno, 2009)

Ceramic membrane materials	Polymeric membrane materials
High production cost	Low production cost
Fragile, difficult to handle	Flexible, easy to handle
Complex production scale-up	Straightforward production scale-up
Difficult variation of form and shape	Easy variation of form and shape
Good long term stability	Short life time, bad long term stability
Good versatility in organics	Limited versatility in some organics
Thermal regeneration possible	Thermal regeneration impossible
Stable in extreme pH conditions	Limited stability in extreme pH conditions

1.1.3. Membrane preparation via phase inversion

Phase inversion represents one of the most versatile, economical and reproducible fabrication techniques for integrally skinned asymmetric membranes, which entails a controlled change in the polymer phase from liquid to solid (Vandezande, Gevers & Vankelecom, 2008). There are several methods to induce phase inversion (Table 1.2), but in all of them a liquid polymer solution is precipitated into two phases: a solid, polymer rich phase that forms the matrix of the membrane and a liquid, polymer poor phase that forms the membrane pores (Baker, 2004).

Table 1.2 – Phase inversion procedures (Baker, 2004)

Procedure	Process
Water precipitation (the Loeb-Sourirajan process)	The cast polymer solution is immersed in a non-solvent bath (typically water). Absorption of water and loss of solvent cause the film to rapidly precipitate from the top surface down
Water vapour absorption	The cast polymer solution is placed in a humid atmosphere. Water vapour absorption causes the film to precipitate.
Thermal gelation	The polymeric solution is cast hot. Cooling causes precipitation
Solvent evaporation	A mixture of solvents is used to form the polymer casting solution. Evaporation of one of the solvents after the casting, changes the solution composition and causes precipitation

The water precipitation technique, developed by Loeb and Sourirajan in the sixties, is the most commonly used procedure. In their process, precipitation is induced by immersing the cast solution, also known as dope solution, containing 20 to 25 wt% of polymer, in a water bath (Loeb & Sourirajan, 1963). The first step consists in evenly spreading the homogeneous polymer cast solution across a non-woven material with a casting knife. The space between the blade of the knife and the surface forms a precise gap, usually between 50 and 300 μm. The next step involves immersing the polymer in a non-solvent bath (water) causing the fast precipitation of the polymer and consequently the formation of the dense top layer. This dense layer acts as a barrier, slowing down the water access into the following layers, forming the porous structures. This procedure is still used in laboratories, but for industrial scale, large casting machines produce rolls of membrane up to 5 000 m long and 2 m wide (Baker, 2004).

The most commonly used approach to describe the phase inversion process is done by using polymer – solvent – non-solvent diagrams (Figure 1.3), also known as ternary phase diagrams. The diagram consists of an equilateral triangle in which each corner correspond to the components in the dope solution (polymer and solvent) and the phase inversion bath (non-solvent). It also shows two zones corresponding to the miscibility of the components. The first zone is the one-phase region, where all the components are miscible (Figure 1.3 – a) Regions 1, 2 and 3). The second zone, the two-phase region (Figure 1.3 – a) Regions 4 and 5), is where the phase separation takes place and the system separates into a solid phase (polymer-rich) and a liquid phase (polymer-poor). Even though the one-phase region is thermodynamically continuous, it can be divided into three different areas according to the polymer state: 1 – homogeneous solution (viscous polymer casting solution), 2 – a solid gel polymer, and 3 – glassy solid polymer. The transition between regions depends on the polymer. However, it can be generalised that the transition between liquid and gel regions occurs at polymer concentrations of 30 to 40%, and above 90% the polymer gel becomes so rigid that it turns into a solid polymer glass. The two-phase region consists of 4 – a metastable region, and 5 – an unstable region limited by the binodal and spinodal curves respectively (Baker, 2004).

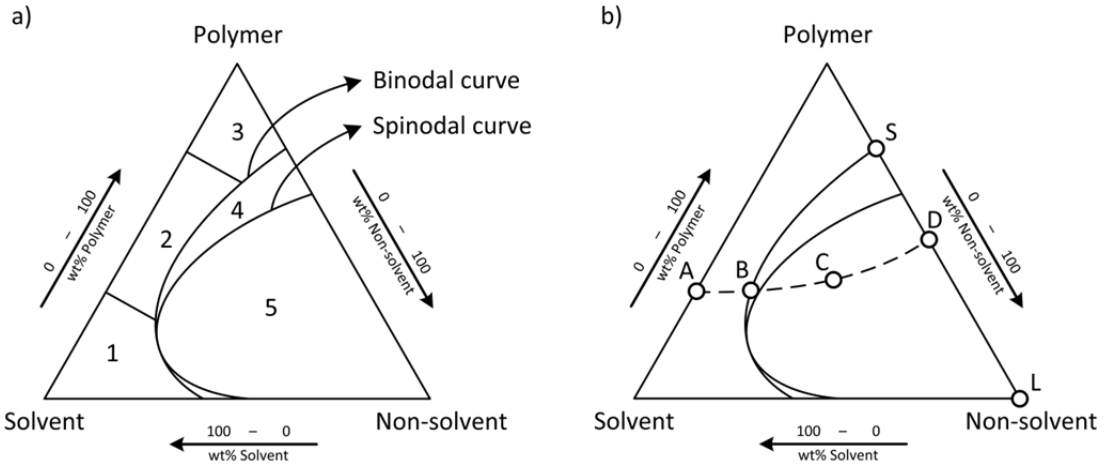

Figure 1.3 – a) Schematic representation of a ternary phase diagram of the phase inversion process; b) Schematic representation of composition variance during membrane formation in a ternary phase diagram. A – initial composition of the dope solution; B – composition at which the polymer starts to precipitate; C – composition at which the polymer can be considered solid; D – final composition of the membrane; S – polymer solid phase; L – polymer liquid phase (Baker, 2004)

During membrane formation (Figure 1.3 - b), via phase inversion, solvent exchange occurs with the precipitation medium, and the initial composition of the dope solution, A, changes according to the dashed line in Figure 1.3 – b), until the final composition of the membrane, D, is obtained. At composition D, the two phases are in equilibrium: a solid phase (polymer rich), S, which forms the final structure of the membrane, and a liquid phase (polymer-poor), L, which embodies the membrane pores filled with non-solvent. The position of D on the S-L line determines the overall porosity of the membrane. The point B corresponds to the point at which the polymer starts to precipitate. As precipitation proceeds, solvent is lost, and non-solvent is absorbed by the solid phase, increasing its viscosity. At C, the viscosity is high enough for the polymer to be considered solid (Baker, 2004).

When the cast polymer film, A, gets in contact with the precipitation medium, the surface begins to precipitate first. In composition B, the surface precipitates quickly, and the two phases formed, do not have time to agglomerate, producing a finely microporous structure. When composition C is reached, the top layer of the film becomes a solid barrier, slowing down the loss of solvent and the admission of non-solvent inside the pores. This leads to a decrease in the precipitation velocity from the top to the bottom of the film, and consequently to an increase of the average pore size, since the two phases formed have more time to separate. The final membrane is formed when composition D is attained, and solvent has been completely replaced by the non-solvent (Baker, 2004).

a) Choice of solvent/non-solvent system. Depending on the solvents and non-solvents used for casting, two types of demixing may take place according to the kinetics of the process – instantaneous and delayed demixing (Figure 1.4). After immersing the membrane in the precipitation medium, in the case of instantaneous demixing (Figure 1.4 - a)), at a specific time t, the top (Figure 1.4 - point 1) and middle (Figure 1.4 - point 2) layers of the membrane, enter almost immediately in the unstable region of the ternary phase diagram, resulting in a finely porous microstructure. On the other hand, when delayed demixing is present (Figure 1.4 - b)) the polymer composition is still located in the

thermodynamically stable region of the diagram, originating a tighter membrane. Phase separation will only occur after more non-solvent enters the film (Vandezande, Gevers & Vankelecom, 2008).

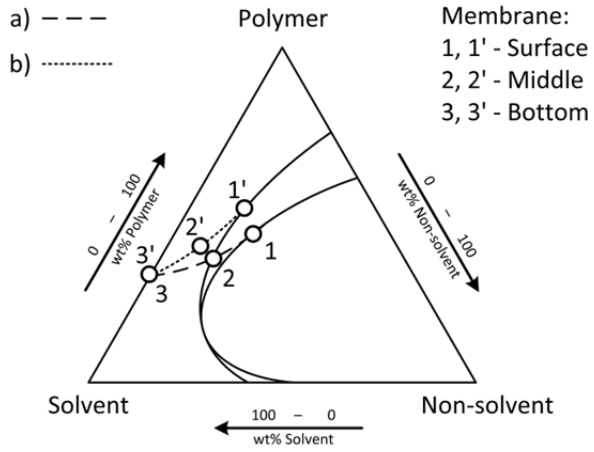

Figure 1.4 – Schematic representation of two different composition pathways across the polymer film, at a time t, almost immediately after immersion in the non-solvent. a) instantaneous demixing; b) delayed demixing (Vandezande, Gevers & Vankelecom, 2008)

b) Polymer concentration. The concentration of polymer in the dope solution, will also affect the membrane morphology and therefore its performance. Increasing the polymer concentration in the dope solution will make the membrane denser, forming accordingly a thicker skin layer with concealed macrovoids in the sublayers, while decreasing the polymer concentration in the dope solution will contribute to a porous structure with macrovoids. Macrovoids are finger- or tear-like pores that can extend over the entire membrane thickness, and are generally considered undesired, since they cause mechanically weak spots in the membrane (Baker, 2004).

c) Co-solvents and other additives. The membrane structure differs with the composition of the dope solution. The addition of a volatile co-solvent to the casting solution will increase the polymer concentration in the top layer during phase inversion, producing a membrane with lower throughput and higher rejection (Vandezande, Gevers & Vankelecom, 2008). Other additives such as inorganic salts, pore forming agents, other non-solvents or low molecular weight polymers can be added to the dope solution. These agents, even in small amounts, can have significant repercussion on the membrane structure and consequently on its performance (Pinnau & Freeman, 2000).

1.1.4. Post-treatment and conditioning techniques

There are many parameters that influence solute separation. One of them is the post-formation treatment which has a severe impact on the final structure of the membrane and its performance. Crosslinking, thermal annealing, solvent exchange and impregnation are some of the most common post-treatment and conditioning techniques used to enhance membrane performance and long-term stability (Mulder, 1996; Baker, 2004; Vandezande, Gevers & Vankelecom, 2008).

a) Crosslinking. In order to improve the chemical, mechanical and thermal stability of asymmetric membranes, it is possible to connect two or more chains to each other via crosslinking (Figure 1.5).

Crosslinking of the polymer is induced using a chemical reaction or through radiation and can be done during membrane formation or after which is the most common procedure. This post formation treatment changes the properties of the polymer, i.e. the polymer becomes insoluble in solvents in which it was soluble before. Further, crosslinking results in membranes which reject lower MW solutes. However, this is often at the expense of a decrease in membrane permeance (Mulder, 1996).

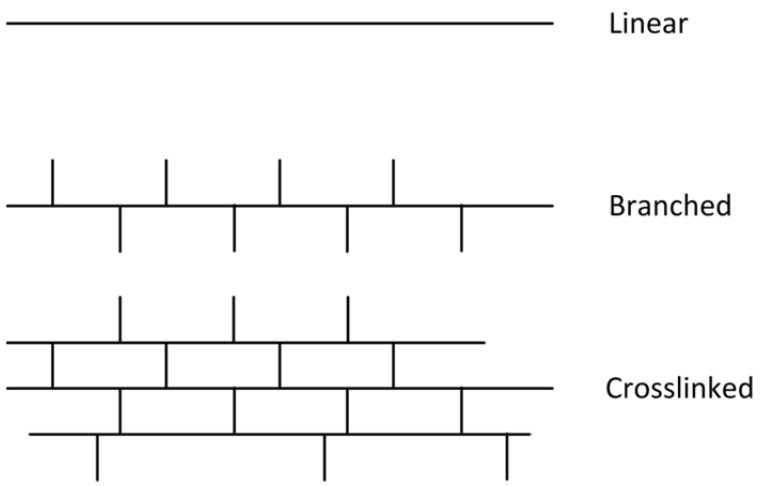

Figure 1.5 – Schematic representation on how to build up macromolecules (Mulder, 1996)

b) Thermal annealing. A commonly used technique to obtain tighter nanofiltration membranes is thermal annealing, i.e. heating up the membrane to temperatures below the degradation temperature of the polymer. However, with this kind of treatment, the permeance of the membrane decreases. This is due to the fact that the polymer chains reorganise themselves to a more stable thermodynamic structure (See-Toh, Ferreira & Livingston, 2007). A gradual loss of porosity in the top layers is also verified, as well as significant shrinkage of the membrane structure (Vandezande, Gevers & Vankelecom, 2008).

c) Solvent exchange and impregnation. Asymmetric membranes can be stored wet (water, alcohol) or dried (impregnated), the latter being the most common method. The obtained membranes are usually dried by a multiphase solvent exchange. The residual non-solvent present in the membrane after immersion is replaced by a solvent, miscible with the non-solvent and more volatile, easier to be removed via evaporation. In order to improve the performance, flexibility and handling of asymmetric membranes, they can be impregnated with conditioning agents, which must be inert to the polymer and non-volatile, such as polyethylene glycol (PEG), polymethylsiloxane (PMS) or glycerol. This process minimises the risk of pore collapsing upon drying, avoiding therefore loss of the original structure and handling issues (Vandezande, Gevers & Vankelecom, 2008).

1.1.5. Membrane processes

Membrane processes are characterised by the use of a membrane to obtain a certain separation. Certain solutes are transported more willingly through the membrane than others due to physical and/or chemical properties between the membrane and the permeating components. Solvent/solute transport through the membrane occurs as a result of gradients in pressure (ΔP), concentration (ΔC), temperature (ΔT) or electrical potential (ΔE) (Table 1.3) that generate a driving force (Mulder, 1996).

Table 1.3 – Membrane processes according to their driving forces (Mulder, 1996)

Pressure (ΔP)	Concentration (ΔC)	Temperature (ΔT)	Electrical potential (ΔE)
Microfiltration	Gas separation	Thermo-osmosis	Electrodialysis
Ultrafiltration	Vapour permeation	Membrane distillation	Membrane electrolysis
Nanofiltration	Pervaporation		
Reverse osmosis	Dialysis		
	Diffusion dialysis		
	Membrane contactors		

Microfiltration (MF), ultrafiltration (UF), nanofiltration (NF) and reverse osmosis (RO) are the most important pressure driven membrane processes and the difference between them is regarding the particle size of the solutes to be separated. All of them are used to purify or concentrate a dilute (aqueous or non-aqueous) solution. Higher pressures are applied as we go from microfiltration to reverse osmosis (Table 1.4). Since the size of the particles to be separated decreases form microfiltration to reverse osmosis, the resistance of the membranes to mass transfer increases accordingly (Mulder, 1996).

Table 1.4 – Pressure driven membrane processes (Mulder, 1996)

Membrane process	Pressure range (bar)	Pore sizes (nm)	Separation type
Microfiltration (MF)	0.1 – 2.0	> 100	Particles
Ultrafiltration (UF)	1.0 – 5.0	1 – 100	Macromolecules
Nanofiltration (NF)	5.0 – 20	< 2	Low molecular weight solutes
Reverse osmosis (RO)	10 – 60		

Nanofiltration is a membrane process in which the pore range of the membrane is generally within 0.5 – 2 nm, and which can selectively separate molecules in the region of 200 – 2000 $g.mol^{-1}$ (Da, Daltons). It has been applied to aqueous filtrations, but due to lack of suitable solvent stable membranes has not been widely applied to the separation of solutes in organic solvents.

Nevertheless, organic solvent nanofiltration (OSN), or solvent resistant nanofiltration (SRNF), has great potential for industrial applications such as solvent exchange (Sheth, Qin, Sirkar, *et al.*, 2003), catalyst recovery and recycling (van der Gryp, Barnard, Cronje, *et al.*, 2010), purifications and concentrations (Van der Bruggen, Mänttäri & Nyström, 2008; Vandezande, Gevers & Vankelecom, 2008).

1.1.6. Membrane performance characterisation

Membrane characterisation is not only based on physical parameters (pore size and distribution, surface roughness and overall membrane thickness) and chemical parameters (charge and hydrophobicity), but is also based on functional performance. Membrane performance is characterised by filtration experiments, and two features are measured – permeance and separation. The permeance ***B*** ($L.m^{-2}.h^{-1}.bar^{-1}$) is defined as the volume permeated, V_p (L), per unit membrane area, A (m^2), per unit time, t (h), per unit pressure drop, ΔP (bar). In general, the flux ***J*** ($L.m^{-2}.h^{-1}$) is measured (Equation 1.1) at a given pressure ΔP and hence, the permeance can be calculated (Equation 1.2). Parameters like temperature and solute concentration have an impact on the flux of NF membranes. The permeation flow tends to increase with higher temperatures because of reduction of solvent viscosity and increased polymer chain mobility. Higher solute concentrations result in decreased flux due to increase of osmotic pressure and therefore, decrease of the driving force.

Equation 1.1

$$J = \frac{V_p}{A.t}$$

Equation 1.2

$$B = \frac{J}{\Delta P}$$

The rejection ***R*** (%) of a solute ***i*** will determine the membrane separation ability and is described by the following equation (Equation 1.3),

Equation 1.3

$$R = \left(1 - \frac{c_{i,P}}{c_{i,F}}\right) x\ 100$$

where $c_{i,P}$ is the concentration of the molecule ***i*** in the permeate and $c_{i,F}$ the concentration of the molecule ***i*** in the feed. If a series of solutes is used for filtration purposes the rejection of each component can be calculated and plotted. By plotting the rejections of solutes with different molecular weight (MW) it is possible to obtain another important parameter, which is the molecular weight cut-off (MWCO), defined as the lowest molecular weight solute that is 90% retained by the membrane (Figure 1.6).

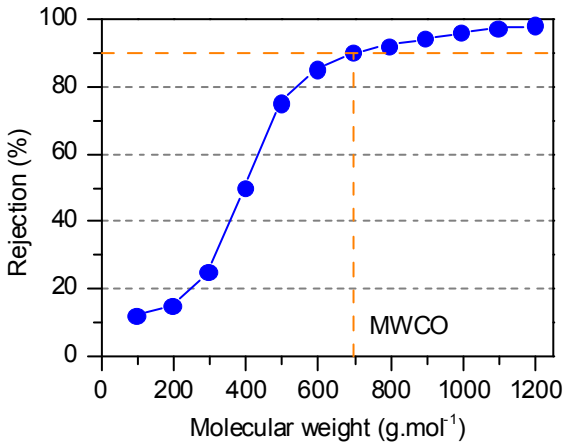

Figure 1.6 – Schematic representation of a rejection profile of a typical OSN membrane with indication of the MWCO (Mulder, 1996)

1.1.7. Transport in membranes

In order to understand and predict the behaviour of a specific membrane, several mathematical models were developed. Three groups of mathematical models are accepted to describe transport through membranes. The first group of models is based on irreversible thermodynamics, treating the membrane as a black-box, while the other two, the pore-flow and the solution diffusion models, take into account properties from the membrane itself (Vandezande, Gevers & Vankelecom, 2008).

The most reliable transport models for OSN are the pore-flow (Figure 1.7 - a)) and the solution-diffusion (Figure 1.7 - b)) models, which describe the transport through porous (e.g. micro- and ultrafiltration membranes) and dense membranes (e.g. reverse osmosis, gas separation and pervaporation membranes) respectively since NF is a process intermediate between UF and RO (Van der Bruggen, Mänttäri & Nyström, 2008; Baker, 2004).

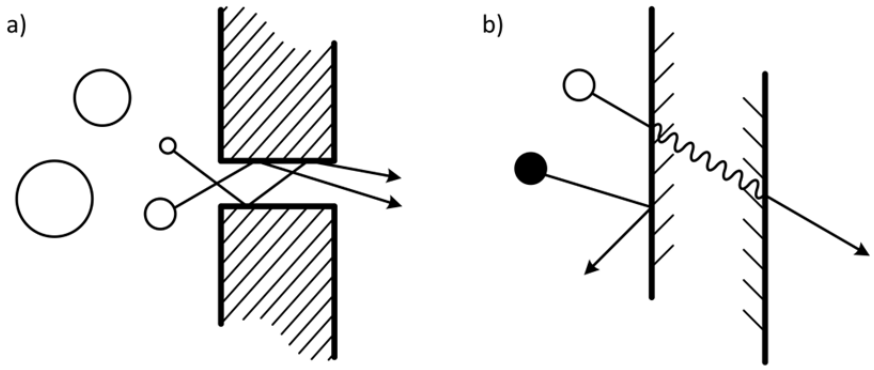

Figure 1.7 – Mass transport through membranes can be described by a) flow through membrane pores in microporous membranes; or by b) the solution-diffusion mechanism through the membrane material in dense membranes (Baker, 2004)

Both models are based on mass transfer principles, however different assumptions are made. According to the pore-flow model, the concentration of species across the membrane is constant and

the transport is a pressure-driven convective flow through the pores of the membrane (Figure 1.7 - a)). On the other hand, according to solution-diffusion model, the pressure is assumed to be constant across the membrane, and the solute transport occurs by dissolution of the solute in the membrane material and its diffusion due to a concentration gradient (Figure 1.7- b)) (Baker, 2004). The transport through NF membranes can be predicted with these two models since it is considered to be in a transition region, between RO and UF (Baker, 2004).

1.2. OSN – an emerging technology

Typical purification processes employed at industrial scale are distillation, chromatography, adsorption and crystallisation. However, these processes have high energy consumption or lead to partial material degradation. OSN has emerged as a new solution with potential for several industrial sectors. Molecular scale separations using membranes are now a reality, and several companies are investing in membrane technology in order to make it more widely available (Vandezande, Gevers & Vankelecom, 2008).

1.2.1. Membrane applications in organic solvents

Although it is relatively new, OSN has already been applied in several industrial fields - chemical purification (Székely, Bandarra, Heggie, *et al.*, 2012), petrochemical industry (White, 2006), solvent recovery (Rundquist, Pink, Vilminot, *et al.*, 2012), catalytic reactions (van der Gryp, Barnard, Cronje, *et al.*, 2010), solvent exchange (Sheth, Qin, Sirkar, *et al.*, 2003), peptide synthesis (Reddy, Kawakatsu, Snape, *et al.*, 1996), stereochemistry (Ferreira, Macedo, Cocchini, *et al.*, 2006) and membrane bioreactors (Valadez-Blanco, Ferreira, Jorge, *et al.*, 2008).

OSN is changing the way reactions, separations and recycling are approached in industry. Thus, hybrid processes between conventional separation techniques and OSN offer new and greener solutions (Vandezande, Gevers & Vankelecom, 2008).

1.2.2. Polymers generally used for OSN membranes

Membrane performance in OSN conditions depends on the polymers used for membrane formation. These polymers must be resistant to a broad range of solvents and must not dissolve in them. Most polymers are not intrinsically stable in certain solvents, but can be stabilised via crosslinking. Several polymers have shown good performances in OSN processes such as polyimide (PI), polyacrylonitrile (PAN), polyetheretherkethone (PEEK) and others (Vandezande, Gevers & Vankelecom, 2008).

Polyimide (PI). The majority of OSN membranes are integrally skinned asymmetric membranes made of polyimides. These membranes have shown good performances in several organic solvents like toluene, methanol, ethyl acetate and others. When crosslinked with diamines these membranes are stable in polar aprotic solvents, in which polyimides are soluble, such as dichloromethane (DCM),

tetrahydrofuran (THF), *N,N*-dimethylformamide (DMF) and *N*-methylpyrrolidone (NMP) (See Toh, Lim & Livingston, 2007).

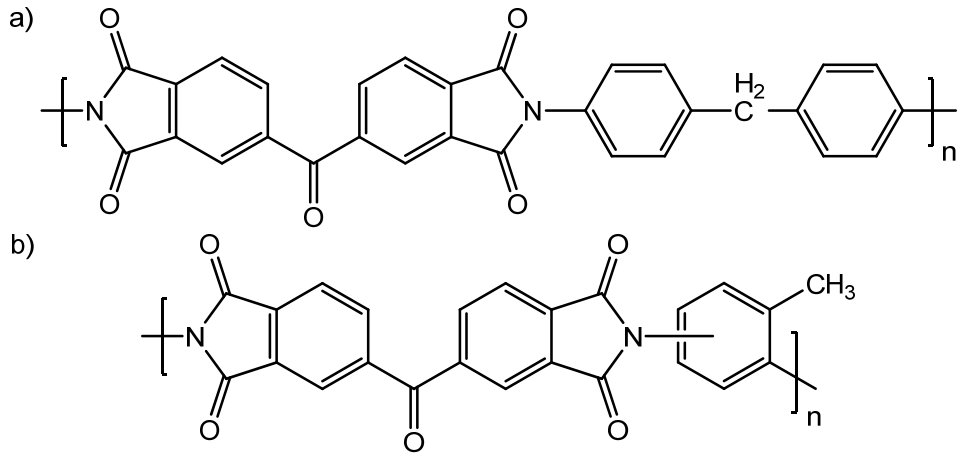

Figure 1.8 – Chemical structure of polyimide Lenzing P84 - 20% of a) methylphenylenediamine (MDI) and 80% of b) toluenediamine (TDI) (See-Toh, Ferreira & Livingston, 2007)

Polyacrylonitrile (PAN). PAN membranes have been widely used in water treatment, pervaporation, enzyme immobilization and biomedical applications (Wu, Wan & Xu, 2012). These membranes have shown thermal stability (up to 130 °C) and resistance to many organic solvents (Zhao, Li, Wang, *et al.*, 2005). PAN has also good resistance against chlorine, and cleaning agents. Nevertheless, the applications of PAN membranes have been hindered by the brittleness of the membrane and pore collapse upon drying (Jung, Yoon, Kim, *et al.*, 2004).

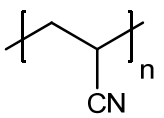

Figure 1.9 – Chemical structure of polyacrylonitrile (Vandezande, Gevers & Vankelecom, 2008)

Polyetheretherkethone (PEEK). PEEK membranes are used as supports for composite ultrafiltration and reverse osmosis membranes. This polymer has a high melting point (about 367 °C) and a moderate glass transition temperature (about 145 °C), low solubility and high chemical resistance to acids and bases, except to strong acids in high concentrations, which is an advantageous property for a membrane for OSN. PEEK is soluble in concentrated sulphuric acid at room temperature (Bishop, Chau, Koo, *et al.*, 1991) and further crosslinking is not required, making this polymer attractive for OSN. However, the fact it is only soluble in sulphuric acid, arises casting problems. Modified PEEK has been developed to make it soluble in common solvents, but at the expense of the need of crosslink it, introducing another step to the membrane preparation (Hendrix, Van Eynde, Koeckelberghs, *et al.*, 2013).

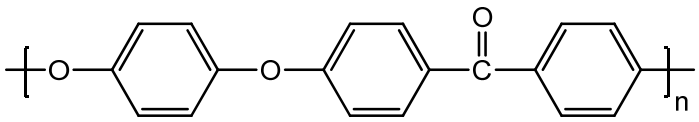

Figure 1.10 – Chemical structure of polyetheretherkethone (Vandezande, Gevers & Vankelecom, 2008)

1.2.3. Polybenzimidazole (PBI) as OSN membrane material

In order to implement OSN to relevant processes, membranes must be resistant to several solvents, temperature and pH environments. Inorganic materials are ideal for these conditions since they are not chemically or structurally affected by organic solvents, acids and bases. However, as it was mentioned before, they are hard to produce and handle, and are more expensive to synthesise when compared to organic membranes. Organic membranes, made out of polymeric materials, have been trying to overcome these problems (Baker, 2004; Drioli & Giorno, 2009; Vandezande, Gevers & Vankelecom, 2008). New materials are being developed, new crosslinking reactions are being study and novel processes are being considered in order to overcome these problems (Van der Bruggen, Mänttäri & Nyström, 2008).

Polybenzimidazole is an amorphous thermoplastic polymer containing benzimidazole rings in its repeating unit (Li, He, Jensen, *et al.*, 2004). The most commonly used polybenzimidazole is poly-2,2-(m-phenylene)-5,5-bibenzimidazole (PBI) due to its outstanding thermal (T_g = 425-436 ºC), mechanical (retention of stiffness and toughness) and chemical stability (towards solvents, acids and bases) in corrosive environments (Chung, 1997). PBI has been studied extensively for reverse osmosis (Sawyer & Jones, 1984) gas separation (Kumbharkar, Karadkar & Kharul, 2006), aqueous NF (Wang, Xiao & Chung, 2006), fuel cells (Li, He, Jensen, *et al.*, 2004) and more recently for OSN (Livingston & Bhole, 2013). PBI is soluble in polar aprotic solvents as *N,N*-dimethylacetamide (DMAc), *N*-methylpyrrolidinone (NMP) and dimethylsulfoxide (DMSO), and can be dissolved and cast from solutions of them. For filtration in such solvents, PBI must be crosslinked with aliphatic dihalogenes (Livingston & Bhole, 2013) or xylene dihalogenes (Wang, Xiao & Chung, 2006) to prevent polymer dissolution and membrane failure. Using PBI for the preparation of OSN membranes could overcome some of the issues that other polymers have, e.g. easy to process into flexible flat sheet membranes, great chemical resistance in corrosive environments and hydrophilic properties.

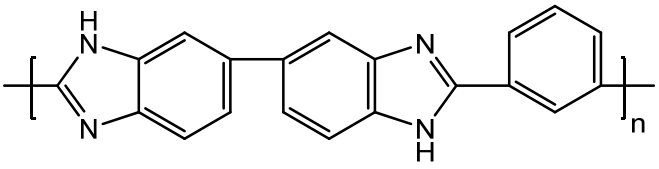

Figure 1.11 – Chemical structure of poly-2,2-(m-phenylene)-5,5-bibenzimidazole (PBI) (Chung, 1997)

Controlling PBI MWCO – learning from polyimide. Polyimide membranes are commonly prepared via phase inversion, and effect of polymer concentration and the solvent/co-solvent ratio have been

found to strongly influence the molecular weight cut-off (MWCO) and flux of PI membranes (See-Toh, Silva & Livingston, 2008; Vandezande, Li, Gevers, *et al.*, 2009; Soroko, Lopes & Livingston, 2011; Soroko, Makowski, Spill, *et al.*, 2011). However, until now, a methodology to describe thermodynamics of quaternary polymer solutions (polymer, solvent, co-solvent and the non-solvent) has not been developed (Soroko, Lopes & Livingston, 2011).

Solubility parameters can determine, to a certain degree, the interactions between the components in the dope solution; i.e. polymer–solvent, polymer–non-solvent and solvent–non-solvent (Strathmann & Kock, 1977) and those interactions are known to affect the course of the phase inversion (See-Toh, Silva & Livingston, 2008). The Hildebrand solubility parameter, later improved by Hansen, is a measure of the intermolecular energy (Gedde, 1995; Barton, 1983). Hansen solubility parameter takes into account dispersion forces, polar forces and hydrogen bonding, and is composed of three partial solubility parameters; $\Delta\delta_{P/S}$, $\Delta\delta_{P/NS}$ and $\Delta\delta_{S/NS}$ (Barton, 1983).

The first, $\Delta\delta_{P/S}$, represents the affinity between polymer and solvent. When the polymer is dissolved in a thermodynamically “suitable” solvent, polymer-solvent contact is favoured and polymer chains are relatively extended, whereas in a “poor” solvent the polymer chain aggregation is higher (Billmeyer, 1984). This aggregation makes the dope less stable, and during immersion into the non-solvent bath, the solvent between polymer aggregates can leave faster, leading to a denser top layer formation. The second one, $\Delta\delta_{P/NS}$, is related to polymer and non-solvent interactions. Higher $\Delta\delta_{P/NS}$ implies lower affinity between polymer and the non-solvent leading to a decreased miscibility region, favouring instantaneous demixing and consequently a more open membrane. Lastly, $\Delta\delta_{S/NS}$, regards the solvent/non-solvent exchange rate during immersion. Higher values of $\Delta\delta_{S/NS}$, represent low affinity between solvent and non-solvent inducing a slow in-diffusion of the non-solvent into the polymer film, causing delayed demixing, and consequently leading to the formation of a tighter skin layer. It is then expected, that an increase of $\Delta\delta_{P/S}$ and $\Delta\delta_{S/NS}$, and a decrease of $\Delta\delta_{P/NS}$ results in the formation of a tighter membrane (Soroko, Lopes & Livingston, 2011). The combination of all solubility parameters leads to a total solubility parameter, $\Delta\delta_t$. Higher $\Delta\delta_t$ is expected to be related with the formation of tighter membranes when compared to lower $\Delta\delta_t$ (Soroko, Lopes & Livingston, 2011).

Soroko, *et al.*, added 1,4-dioxane as a co-solvent in PI dope solutions with different polyimides. Different ratios of solvent/co-solvent (DMF/1,4-dioxane) were tested; 3/1, 1/1 and 1/2 (Soroko, Lopes & Livingston, 2011). The addition of 1,4-dioxane led to the formation of tighter membranes with higher rejections with the majority of polyimide membranes. These results were in accordance with the total solubility parameter theory described above. Other experiments were conducted with different solvent/co-solvent systems, NMP/THF, and the results were once again quite consistent with the predictions from the total solubility parameter, except for one polyimide membrane, that had a higher $\Delta\delta_t$ value and a lower rejection with DMF/1,4-dioxane 3/1 when compared to the membrane prepared with NMP/THF 3/1, with lower $\Delta\delta_t$ and higher rejection (Soroko, Lopes & Livingston, 2011).

1.3. Challenges in OSN and research motivation

1.3.1. Strengths and limitations of OSN membrane processes

There are numerous attractive features in OSN membrane processes. In most cases, membrane separation processes have low energy consumption comparing with other unit operation like distillation or crystallisation. Thermal damage that leads to degradation or side reactions is minimised due to the low temperature of operation, when compared to distillation processes. No phase transition takes place and no expensive additional equipment is required besides the membrane module and the high pressure pump in the majority of the processes. Therefore, membrane processes are generally considered environmentally sustainable and cost-effective processes (Vandezande, Gevers & Vankelecom, 2008).

Membrane processes are versatile, in the sense of being able to adjust to different applications such as water purification, carbon capture or organic solvent exchange. It is relatively simple to scale-up, and can be easily combined with other processes into a hybrid process (Vandezande, Gevers & Vankelecom, 2008).

Despite these advantages, only a few large-scale OSN processes are running. The most relevant limitations in OSN are related to low membrane stability in a wide range of organic solvents and non-reproducible performances at long term operation. Membrane compaction, insufficient separation, concentration polarisation and fouling of the membrane surface are also some of the challenges that OSN is still struggling with (Vandezande, Gevers & Vankelecom, 2008). The lifetime of OSN membranes depends mostly on the compatibility between the membranes and the solvents used. It is common to observe interactions between polymeric membranes and organic solvents leading to swelling, deformation or dissolution of the membrane to a certain extent (Van der Bruggen, Mänttäri & Nyström, 2008). Crosslinking the membranes can minimise these problems (See Toh, Lim & Livingston, 2007).

Fouling problems are related to the deposition of retained solutes in the membrane due to adsorption leading to precipitation, cake formation and pore blocking (Mulder, 1996). Concentration polarisation is an important fouling mechanism in which a higher concentration of solutes is created next to the membrane boundary layer, when compared to the bulk solution. This is owing to the accumulation of solutes at the membrane surface (Vandezande, Gevers & Vankelecom, 2008). This causes a reduction in the driving force solvent transport, resulting in a decreased permeate flux and increased mass transfer resistance (Mulder, 1996). It is possible to decrease the concentration polarisation or fouling effect by increasing the cross-flow velocity, using pulsate flow or ultrasound treatment (Mulder, 1996; Vandezande, Gevers & Vankelecom, 2008).

In OSN, relatively high pressures are applied and compaction of the pores in the polymeric membrane matrix is observed (Mulder, 1996; See-Toh, Silva & Livingston, 2008). The flux of the membrane declines until a steady state is reached, i.e. no reduction in flux is observed. At the same time solute

rejection increases before stabilisation is obtained (Gibbins, D' Antonio, Nair, *et al.*, 2002; Mulder, 1996). In order to minimise this behaviour, polymeric membranes should be conditioned with pure solvent until a steady flux is obtained prior to the actual separation process (Gibbins, D' Antonio, Nair, *et al.*, 2002).

As shown in Figure 1.6, the rejection of OSN membranes is characterised by a sigmoidal curve, which is never completely sharp, resulting in an incomplete separation between compounds with similar molecular weight. This is due to the fact that the pores in OSN membranes have a broad size distribution (Richard Bowen & Doneva, 2000) leading to the presence of molecules in the permeate with size above and below the average pore size of the membrane, being this one of the major limitations for a wider application of membrane processes (Van der Bruggen, Mänttäri & Nyström, 2008). Several solutions are being studied to overcome this problem, like multiple membrane stages or membrane cascades (Kim, Freitas da Silva, Valtcheva, *et al.*, 2013).

1.3.2. Research motivation

For membranes to be applicable in OSN conditions, they must meet several criteria in terms of material, structure and performance. The market of OSN membranes is still quite small and only a few polymeric membranes are available on the market. DuraMem® and PuraMem® are commercially available OSN membranes produced by Evonik. They are both made from P84® polyimide and are stable in non-aqueous solvents. DuraMem® has long term stability in polar aprotic solvents such as acetone, tetrahydrofuran, *N,N*-dimethylformamide and others. On the other hand, PuraMem® has good stability in apolar hydrocarbon-type solvents like toluene, heptane, hexane, methylethylketone and others (Evonik MET Ltd., n.d.). SolSep BV is another producer of membranes. They sell membrane modules that are stable in organic solvents like alcohols, ketones, alkanes and aromatics (SolSep BV - Robust Membrane Technologies, n.d.).

All OSN membranes, commercially available or laboratory developed, still face several challenges though.

Chemical stability. The membrane polymer and the support must be stable in diverse solvents. The polymer has to dissolve in common organic solvents in order to be easily processed, and it must have reactive functional groups to allow further solvent stability improvement.

Mechanical stability. The polymer must originate flexible and defect-free membranes, which can resist operating temperatures and pressure without compromising its performance.

Permeance. NF membranes in general have low permeance. Separations must be time efficient, and a high permeance coupled with high rejections is desired. However, typical NF membranes present a trade-off between rejection and permeance. Compaction during filtration is also a common problem of IS asymmetric membranes.

Selectivity. Ideal membranes would have a sharp selectivity separating completely the target molecules from the undesired compounds, however this is not verified, and research is being conducted to improve the membrane itself, and process optimisation is also being undertaken. Control over the separation performance of OSN membranes is then desirable in order to achieve improved separation.

These challenges have been addressed in many ways, but there is still room for improvement in terms of materials and performance. Little research has been done to understand how membrane formation influences separation performance. In this dissertation, this will be explored by studying multi-component systems in PBI membrane formation. Different co-solvents will be added in the dope solutions, and a relation with total solubility parameters will be studied, following what has been recently done with polyimide membranes.

2. Materials and Methods

In order to better understand the transport through membranes and gain reliable separation data improved membrane characterisation tools are needed (See Toh, Loh, Li, *et al.*, 2007). Characterisation parameters may be regarding morphological or performance features of the membrane (Cuperus & Smolders, 1991). Morphological characterisation combines physical (e.g. pore size, distribution and shape, skin layer thickness or surface roughness) and chemical (e.g. charge density, hydrophylicity or hydrophobicity) parameters, while permeance and rejection describe functional properties of the membrane. Functional parameters are more practical for membrane selection due to the difficulty in relating morphological parameters to membrane performance (See Toh, Loh, Li, *et al.*, 2007).

2.1. Polybenzimidazole membranes

2.1.1. Materials

Celazole® S26 polybenzimidazole (PBI) solution was purchased from PBI Performance Products Inc. (USA). The solution contains 26 wt% polymer and 1.5 wt% lithium chloride (LiCl), a stabiliser, dissolved in *N,N*-dimethylacetamide (DMAc). Non-woven polypropylene (PP) fabric Novatexx 2471 was obtained from Freudenberg Filtration Technologies (Germany). All solvents such as DMAc, *N,N*-dimethylformamide (DMF), 1,4-dioxane (DXN), ethanol (EtOH), propan-2-ol (IPA), acetonitrile (MeCN), methanol (MeOH) and tetrathydrofuran (THF) were HPLC grade and used as received from VWR (UK). The crosslinking agent was α,α'-dibromo-p-xylene (DBX), and polyethylene glycol (PEG_{400}) for membrane impregnation were both from VWR (UK).

2.1.2. Preparation of IS asymmetric PBI membranes

When required, Celazole® S26 was diluted with DMAc to lower polymer concentrations, co/non-solvents were added accordingly for the multi-component study. The dopes were stirred continuously at room temperature until a homogeneous solution was obtained and then left overnight to remove air bubbles. Membranes were cast on a non-woven PP fabric using a bench top laboratory casting machine with adjustable knife set at 250 µm (Elcometer UK). The membranes were then immersed in deionised water precipitation bath at 23 ± 1 °C for 24 h. Following this, the membranes were washed with IPA to remove residual solvent and water.

To crosslink the polymer, the membranes were immersed in a solution containing 3 wt% DBX in MeCN (Figure 2.1), at 80 °C for 24 h under constant stirring and reflux. After the reaction, the membranes were washed with IPA until complete removal of residual crosslinking agent. Following this, the membranes were immersed in a PEG_{400}/IPA solution (1/1 v/v, or different concentrations for the post-treatment study) for 4 h to preserve the pore structure and allow dry storage.

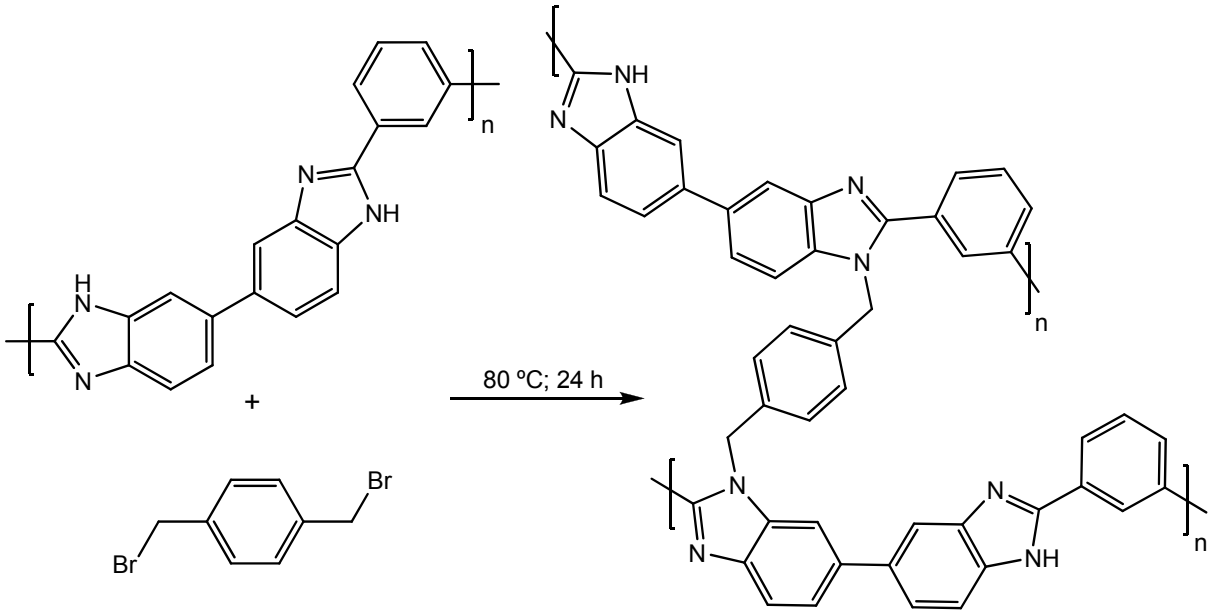

Figure 2.1 – Chemical crosslinking mechanism of 2,2-(m-phenylene)-5,5-bibenzimidazole (PBI) with α,α'-dibromo-p-xylene (DBX)

2.2. Cross-flow filtration system

Membrane selection, in OSN, is usually based on molecular weight cut-off (MWCO) as specified by the manufacturer (U. Razdan, S.V. Joshi & V. J. Shah, 2003). See Toh et al. proposed the use of homologous polymers with steadily increasing molecular weight. Oligomers are ideal for the characterisation of membranes regarding their MWCO due to uniformly increasing monomer units (See Toh, Loh, Li, *et al.*, 2007). A homologous series of styrene oligomers was used allowing to obtain rigorous understanding of the MWCO of the studied membranes, using dead end (Figure 2.2– a)) and cross flow filtration (Figure 2.2– b)) (See Toh, Loh, Li, et al., 2007).

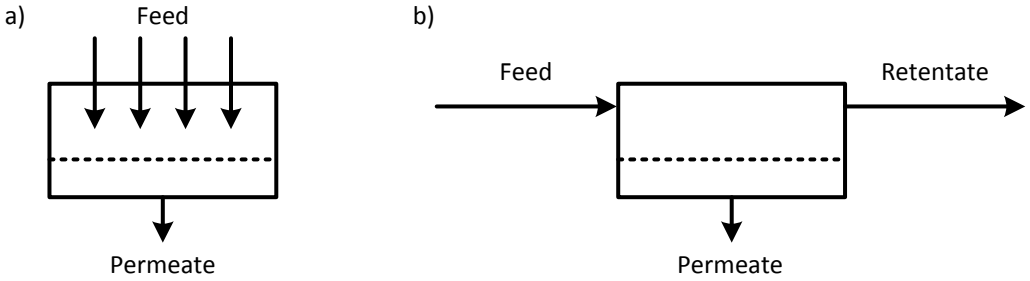

Figure 2.2 – Schematic diagram of separation processes on a membrane: a) dead-end cell and b) cross-flow (Baker, 2004)

Membranes developed in this work, were characterised with polystyrenes (PS) dissolved in acetonitrile (MeCN) (1 $g.L^{-1}$) only in a cross flow system. Dead end filtration is not ideal, due to poorer hydrodynamics when compared with cross flow (Gibbins, D' Antonio, Nair, *et al.*, 2002).

The filtration experiments were carried out in a cross-flow filtration apparatus (Figure 2.3 - left) with eight cross-flow cells (Figure 2.3 - right) connected in series holding membranes with an effective area of 14 cm^2 each. The feed solution was charged into a 5 L feed tank and re-circulated at a flow rate of 100 $L.h^{-1}$ using a diaphragm pump. A flowmeter was used to measure the flow rate, provided by the diaphragm pump. The pressure in the system was measured by a pressure gauge located after the pump, and was regulated with a back pressure regulator. Temperature control was provided by a temperature controller connected to a solenoid valve that regulated the flow of cooling water through the heat exchanger located before the feed tank. Permeate samples were collected from individual sampling ports, and feed samples were taken from the feed sampling port situated before the pump.

Permeance and rejection were calculated according to Equation 1.2 and Equation 1.3 respectively.

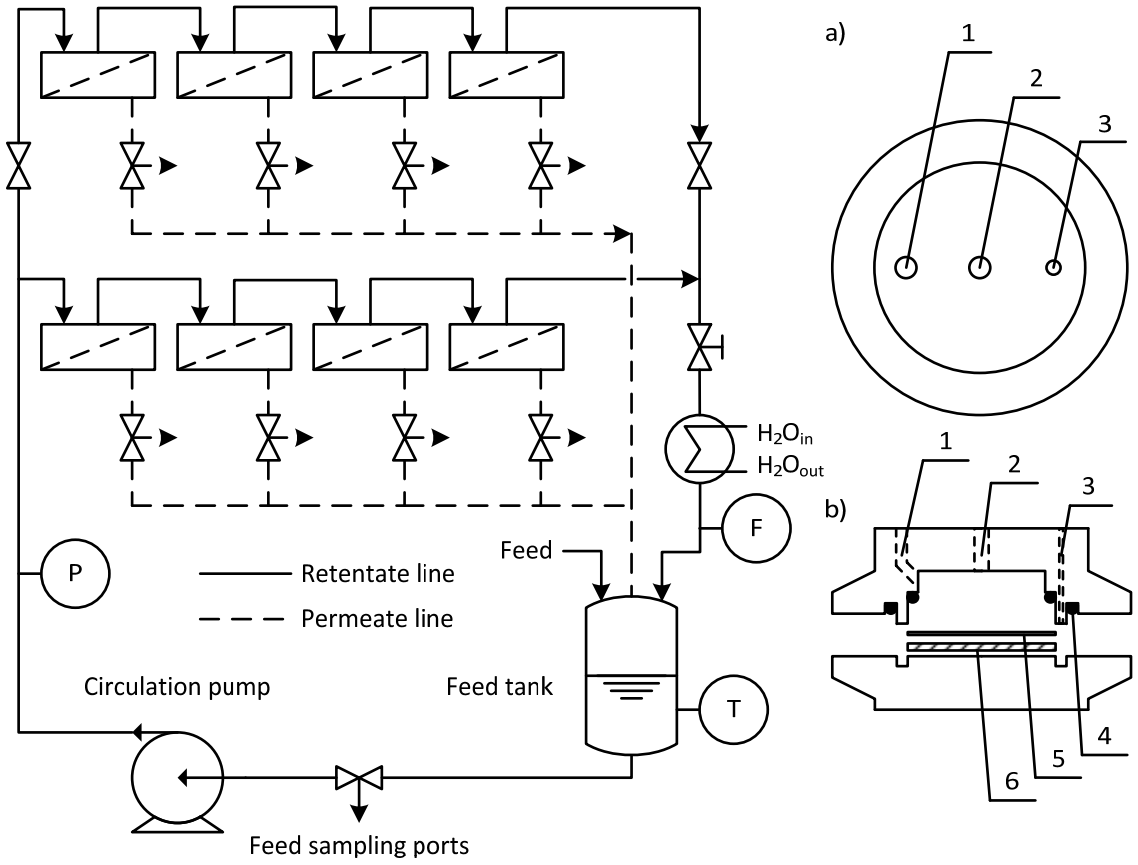

Figure 2.3 – Left - Schematic representation of cross-flow filtration apparatus used for membrane filtrations (P – pressure gauge; F – flow meter; T – thermocouple);
Right - Schematic representation of a filtration cell used for membrane screening in cross-flow conditions; a) top view b) cross section; 1 – Feed port, 2 – Retentate port, 3 – Permeate port, 4 – O-ring, 5 – Membrane coupon, 6 – Sintered disc

2.3. Analytical methods and parameters calculations

2.3.1. Viscosity measurements

The viscosity of the dope solutions was measured using a rotary viscometer from Cannon Instrument Company (Model 2020), with a spindle size 16 suitable for highly viscous solutions. Viscosities were recorded at 20 °C, but with different spindle speeds according to the torque value given by the viscometer. Solutions with higher viscosities needed lower speeds for a more accurate measurement, and vice-versa.

2.3.2. Scanning electron microscopy (SEM)

Scanning electron micrographs of the cross section of membrane samples were taken using a JEOL 5610 LV. In order to remove the impregnated PEG_{400}, the samples were washed with IPA. To prepare the cross section samples, small squares of the membrane were cut and snapped under liquid nitrogen. They were pasted vertically onto SEM sample holders covered with carbon tape. Finally, the samples were sputtered with gold under argon atmosphere (Emitech K550 coater) to ensure the necessary electron conductivity. The SEM was operated at acceleration voltage of 10 kV.

2.3.3. High Pressure Liquid Chromatography (HPLC)

For the analysis of the styrene oligomers (Figure 2.4), an Agilent 1100 Series HPLC system was used. The separation of the oligomers was achieved using an ACE 5-C18-300 column (Advanced Chromatography Technologies, ACT, UK), and a mobile phase of 35 vol% deionised water and 65 vol% tetrahydrofuran, HPLC grade, with 0.1 vol% trifluoracetic acid in each of them was used. The UV detector was set at 264 nm wavelength.

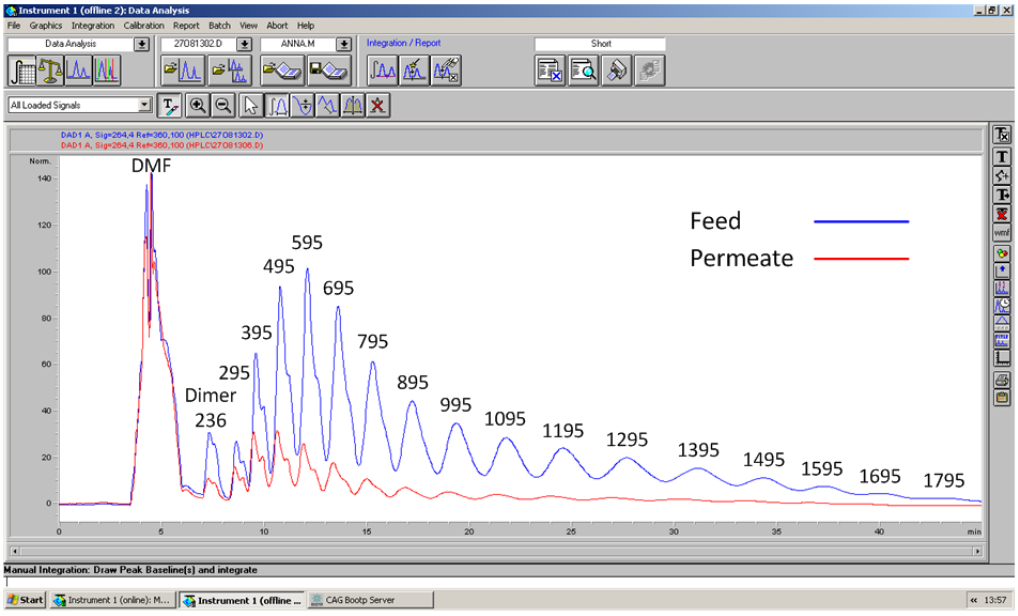

Figure 2.4 – Screenshot of HPLC analysis of PS samples; 1st curve - feed and 2nd curve - permeate

2.3.4. Fourier transform – infrared spectroscopy (FT-IR)

To remove traces of residual chemicals and the impregnated PEG_{400}, membrane samples were first washed with IPA. The samples were fixed on a zinc/selenium diamond plate with the surface facing the beam and infrared spectra were recorded on a Perkin Elmer – Spectrum 100.

2.3.5. Diffusivity parameter

Diffusivity is an important parameter indicative of the diffusion mobility. The higher the diffusivity, the faster diffuse into each other. Equations for predicting diffusivities of liquids are by necessity semi-empirical, since the theory for this not well established as yet. The Wilke-Chang correlation can be used for most purposes where the solvent (A) is diluted in solvent (B) (Geankoplis, 1993). This can be used to calculate and predict the diffusion of the casting solvent in the precipitation bath, e.g. in the water,

Equation 2.1

$$D_{AB} = 1.173 \times 10^{-16}(\varphi M_B)^{1/2} \frac{T}{\mu_B V_A^{0.6}}$$

where T is the temperature in K, M_B is the molecular weight of solvent B in $g.mol^{-1}$, μ_B is the viscosity of solvent B in Pa.s, V_A is solvent A molar volume $m^3.\ g^{-1}.mol^{-1}$, and φ is an "association parameter" of the solvent which is 2.6 for water.

Molar volumes were calculated according to a simple additive estimating method suggested by Schroeder. The rule is to count the number of atoms of carbon, hydrogen, oxygen and nitrogen, add one for each double bond, add the triple bonds multiplied by two, subtract any ring in the component, and multiply the result by seven. The rule is quite accurate with an error of 3.9 % in average. Strongly polar substances (DMAc, DMF and MeCN) have an error greater than 10 % (Poling, Prausnitz & O'Connell, 2001) and therefore their values will not be taken into account in this work.

Equation 2.2

$$V_B = 7\ (N_C + N_H + N_O + N_N + N_{DB} + 2N_{TB} - N_{rings})$$

2.3.6. Total solubility parameter

The solubility parameter δ is a measure for the interaction force between the molecules in a given molecular structure. The closer the solubility parameter values of two components are, the stronger are the interactions between them and the better is their miscibility. The solubility parameter for PBI was calculated with the group contribution method based on the contribution of the structural groups to the cohesion energy E_{coh} ($J.mol^{-1}$) and the molar volume V ($cm^3.mol^{-1}$). The following equation was used to determine δ (Brandrup, Immergut & Grulke, 2004):

Equation 2.3

$$\delta = \sqrt{\frac{\sum E_{coh}}{V}}$$

To calculate the solubility parameter for different solvent mixtures the following equation was used:

Equation 2.4

$$\delta_{S,i,j} = \frac{\sum_{i=1}^{i=n} X_i V_i \delta_i}{\sum_{i=1}^{i=n} X_i V_i}$$

where X_i is the mole fraction, V_i – the molar volume and δ_i – the solubility parameter of a given component i which can be found in literature.

The partial solubility parameters were calculated for the three interactions occurring in the studied system of polymer (PBI), solvent (DMAc and co/non-solvent) and non-solvent (water) – $\Delta\delta_{P/S}$ is related to the polymer/solvent affinity; $\Delta\delta_{P/NS}$ – to the polymer/non-solvent affinity and $\Delta\delta_{S/NS}$ describes the solvent/non-solvent exchange rate during immersion. The following equations were used to calculate the partial solubility parameters:

Equation 2.5

$$\Delta\delta_{P/S} = \left| \delta_P - \delta_S \right|$$

Equation 2.6

$$\Delta\delta_{P/NS} = \left| \delta_{NS} - \delta_P \right|$$

Equation 2.7

$$\Delta\delta_{S/NS} = \left| \delta_{NS} - \delta_S \right|$$

Finally, to calculate the total solubility parameter ($MPa^{1/2}$):

Equation 2.8

$$\Delta\delta_t = \frac{\Delta\delta_{P/S}.\Delta\delta_{S/NS}}{\Delta\delta_{P/NS}}$$

3. Uncrosslinked membranes

3.1. Effect of polymer concentration and pressure

3.1.1. Experimental

In order to control the molecular weight cut-off (MWCO), first we must understand the membrane behaviour without inducing any kind of modification in the dope solution composition, or the membrane post-treatment. Therefore, the first experiments were performed with uncrosslinked polybenzimidazole membranes and consisted in a screening of the membranes performance with different polymer concentrations – 17, 20, 23 and 26 wt% of PBI (Table 3.1). Celazole® S26 was diluted with DMAc to obtain the different polymer concentrations and membranes were prepared in accordance with 2.1.2.

Table 3.1 – Summary of prepared IS asymmetric PBI membranes and the physical characteristics of the dope solutions and casting conditions, for the polymer concentration study

Membrane Code	Polymer concentration (%)	Water T (°C)	Room T (°C)	Room humidity (%)	Viscosity (cP)
17UX(01)	17	22	20	28	4 770
17UX(02)	17	22	20	32	5 560
17UX(03)	17	23	20	36	5 570
20UX(01)	20	20.5	20	28	21 400
20UX(02)	20	24	20	44	19 480
23UX(01)	23	20.5	20	28	67 100
23UX(02)	23	23	20	46	67 700
26UX(01)	26	22	20	28	273 600
26UX(02)	26	23	20	46	249 200

To obtain a better understating of PBI membranes, the experiments in this chapter were conducted during 77 hours during which the pressure was increased in 10 bar intervals and held for 24 hours (Figure 3.1). Finally, the pressure was decreased to 10 bar to allow the evaluation of pressure effect on uncrosslinked PBI membranes.

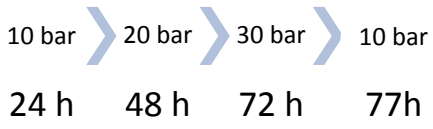

Figure 3.1 – Schematic representation of experimental procedure in chapter 3

Membrane code: e.g. 17UX(01)

- 17 – polymer concentration of 17 wt%
- UX – uncrosslinked polymer
- (01) – batch number 1

3.1.2. Results and discussion

SEM was performed on the membranes to observe how the variation of polymer concentration in the dope solution affects membrane morphology (Figure 3.2). The pictures showed that increasing the concentration of polymer favoured formation of sponge-like structures over macrovoids. Also, it appeared that the top layer and overall membrane thickness increased with increasing polymer content. Consequently, increasing the polymer concentration is expected to result in membranes with high rejection of small MW solutes and low permeance.

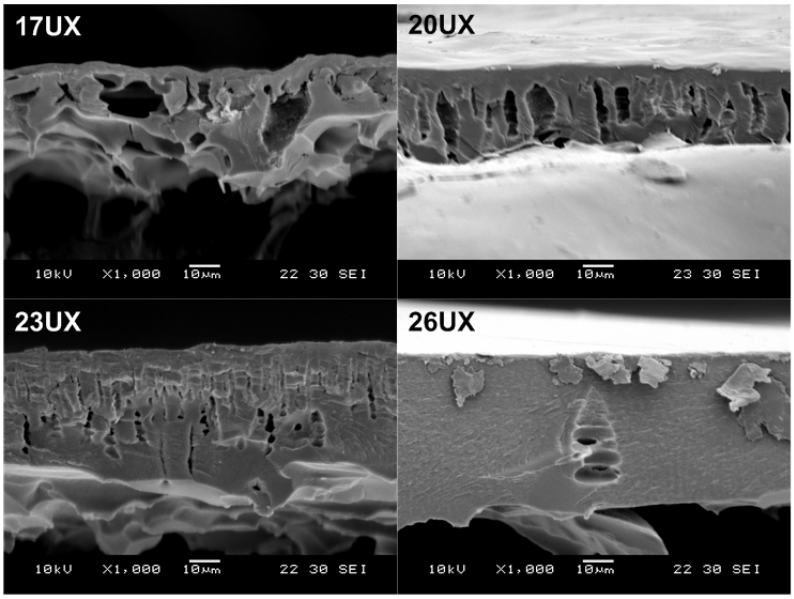

Figure 3.2 – SEM pictures of PBI uncrosslinked membranes 17UX, 20UX, 23UX and 26UX

To study membrane performance, filtration experiments were performed. Permeance (Figure 3.3) and rejection (Figure 3.4) were calculated according to Equation 1.2 and Equation 1.3 respectively.

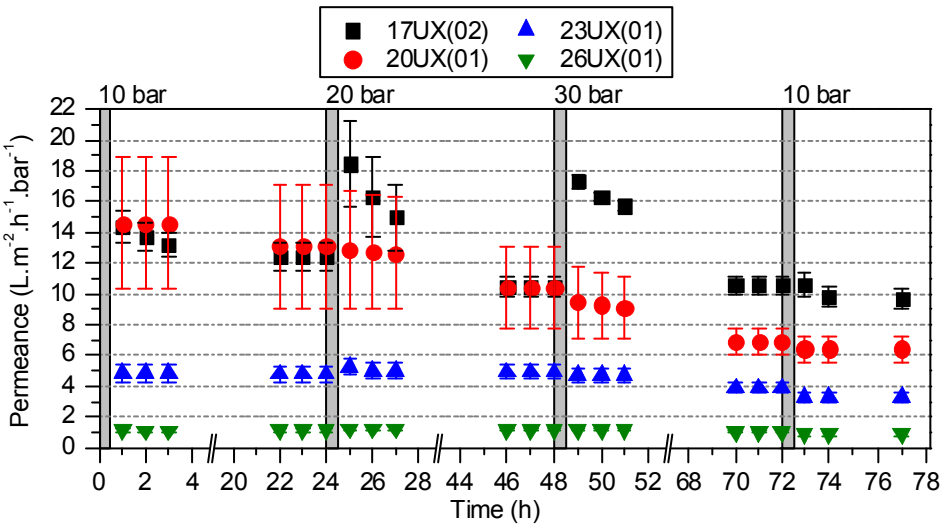

Figure 3.3 – Average PS/MeCN permeance, and standard deviation of uncrosslinked PBI membranes with 17, 20, 23 and 26 wt% polymer concentration, at 30 °C with different pressures, for 77 hours

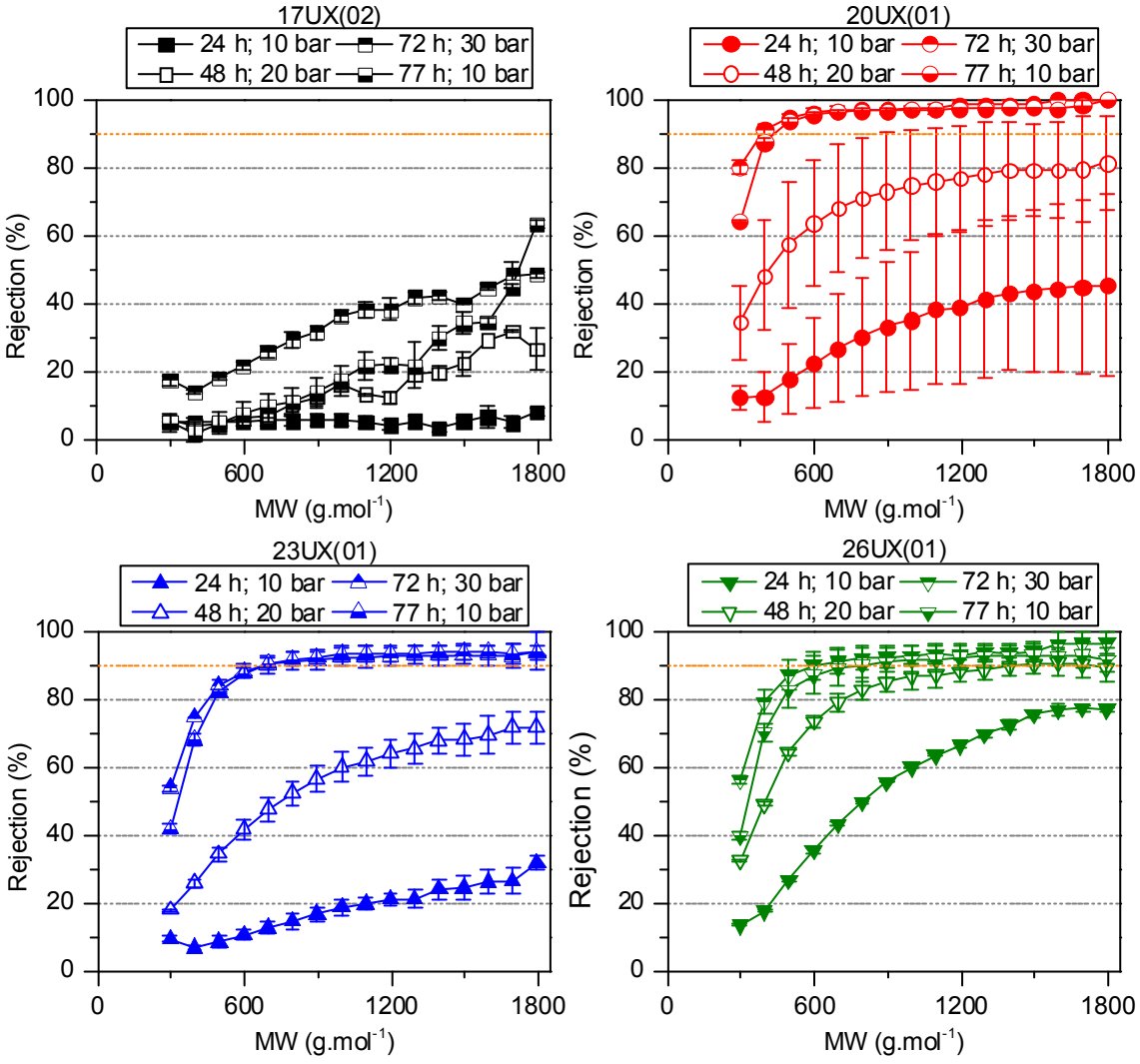

Figure 3.4 – Average PS rejection in MeCN, and standard deviation of uncrosslinked PBI membranes with 17, 20, 23 and 26 wt% polymer concentration, at 30 ºC with different pressures, at 24, 48, 72 and 77 h

During the 77 hours experiment, the permeance decreased in all membranes. There were some fluctuations after each pressure increment, but the permeance would decrease until it stabilised at the respective pressure (Figure 3.3). The permeance was higher in the membranes with lower PBI concentration, confirming what was expected from SEM analysis and literature (Baker, 2004; Mulder, 1996). PS rejection (Figure 3.4) increased over time and since the rejection at 77 hours (10 bar), is much higher than the rejection at 24 hours (10 bar), we can conclude that the polymer chains rearranged when pressure was applied, and do not reorganise upon pressure decrease. This rearrangement is irreversible. It is also possible to observe that this compaction is less pronounced in membranes with higher polymer concentrations (Table 3.2). This effect is likely to be related with the increase of the volume fraction of polymer in the membrane and consequently a lower porosity is obtained, therefore, less free space for the polymer chains to rearrange.

Table 3.2 – Summary of PBI uncrosslinked membranes with different polymer concentrations performance. Initial and final permeances with respective percentage decrease and the MWCO of the tested membranes at 30 bar

Membrane code	Permeance 1 hr, 10 bar ($L.m^{-2}.h^{-1}.bar^{-1}$)	Permeance 77 hr,10 bar ($L.m^{-2}.h^{-1}.bar^{-1}$)	Decrease (%)	MWCO ($g.mol^{-1}$)
17UX(02)	14.4	9.6	33	> 1 800
20UX(01)	14.6	6.4	56	400
23UX(01)	4.9	3.3	33	700
26UX(01)	1.1	0.9	18	700

3.2. Effect of THF addition

3.2.1. Experimental

Following the previous experiment, the multi-component systems study was ready to be initiated. The polybenzimidazole membrane with 17 wt% of polymer proved to have a high permeance and to be more open, meaning that had a higher MWCO, which would allow good resolution of any impact of the co-solvent in membrane performance within the nanofiltration range.

According to Livingston & Bhole, 2012, tetrahydrofuran showed to be compatible as a non-solvent for PBI dope solution preparation. Uncrosslinked PBI membranes containing 17 wt% solids in DMAc/THF (4:1) mixture were prepared and tested in different solvents. The membranes with THF addition showed improved separation of lower MW solutes as compared to the membranes from pure DMAc (Livingston & Bhole, 2012).

Therefore, THF was chosen as the first non-solvent to be tested. The experiments consisted in adding different concentrations of THF to the dope solution and observe the membranes performance. Celazole® S26 was diluted to 17 wt% polymer with DMAc and THF in ratios of 4:1, 4:2 and 4:3

(DMAc:THF) in the dope solutions. Membranes were prepared following the procedure described in 2.1.2.

Membrane code: e.g. 17UX4:1THF(01)

- 17 – polymer concentration of 17 wt%
- UX – uncrosslinked polymer
- 4:1 – DMAc:THF ratio of 4 to 1
- THF – co/non-solvent
- (01) – batch number 1

Table 3.3 – Summary of prepared IS asymmetric PBI membranes and the physical characteristics of the dope solutions and casting conditions, for the addition of THF study

Membrane Code	Non-solvent	Water T (°C)	Room T (°C)	Room humidity (%)	Viscosity (cP)
17UX4:1THF(01)	THF	24	20	42	4 370
17UX4:2THF(01)	THF	24	20	42	4 960
17UX4:3THF(01)	THF	25	20	46	5 440
17UX4:3THF(02)	THF	24	20	40	5 640

3.2.2. Results and discussion

SEM was performed on the membranes to inspect how the addition of THF as a non-solvent to the dope solution affects membrane morphology (Figure 3.5). Pictures showed that membranes cast from dope solutions with higher THF concentration had a more pronounced sponge-like structure with less macrovoids present. It is likely that the addition of THF in the dope solutions induced delayed demixing during phase inversion. As it was explained in 1.1.3 – a), delayed demixing leads to the formation of denser skin layers.

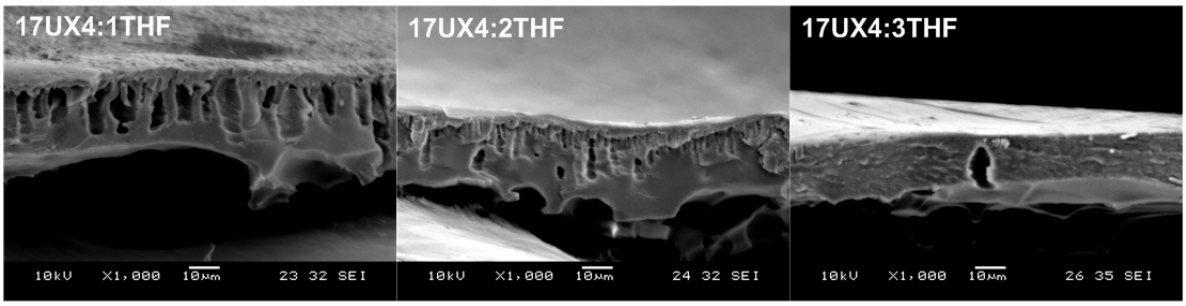

Figure 3.5 – SEM pictures of PBI uncrosslinked membranes 17UX4:1THF, 17UX4:2THF and 17UX4:3THF

The combination of several theories support the idea that THF caused delayed demixing during membrane formation (Table 3.4). THF, is a polar aprotic solvent, but compared to DMAc, also a polar

aprotic solvent, it has a lower polarity index. This means THF has lower affinity to water than DMAc delaying the demixing during the phase inversion. Lower affinity of the non-solvent leads to less macrovoids in membrane structure (Mulder, 1996).

The partition coefficient is also a very useful tool to understand the affinity of solvents to water. This coefficient is the logarithm of the ratio between the concentration of a solute in a mixture of two immiscible hydrophobic (e.g. octanol) and hydrophilic (e.g. water) solvents at equilibrium. Hence, the partition coefficient is a measure of how hydrophilic or hydrophobic a chemical substance is (Leo, Hansch & Elkins, 1971). DMAc has a low partition coefficient, which means, it has high affinity to water (Table 3.4). On the other hand, THF has a positive partition coefficient (Table 3.4), meaning its affinity to water is lower than DMAc. The addition of a solvent with higher partition coefficient as is THF, to the dope solution will delay the demixing process during phase inversion. This means that the two phases (polymer poor and polymer rich) will no longer have time to split, forming less macrovoids across the membrane thickness.

Table 3.4 – Polarity index (Norman B. Godfrey, 1972) and partition coefficient (George Wypych, 2012) of DMAc and THF

Non-solvent	Polarity Index (-)	Partition coefficient (-)
DMAc	6.5	-0.77
THF	4.0	0.46

After calculating, the total solubility parameters for THF as non-solvent in different ratios (Table 3.5), it is possible to observe the same trend Soroko, *et al*. observed with the addition of 1,4-dioxane in PI dope solutions. Increasing the concentration of THF in the dope solution leads to a higher total solubility parameter, and consequently membranes with less macrovoids would be expected, confirming the total solubility parameter theory described in 1.2.3 (Soroko, Lopes & Livingston, 2011).

Table 3.5 – Total solubility parameter of THF as non-solvent in ratios 4:1, 4:2 and 4:3

Non-solvent	$\Delta\delta_t$ (MPa$^{1/2}$)		
	4:1	**4:2**	**4:3**
THF	4.21	4.84	5.31

Finally, according to the polarity index, the partition coefficient and total solubility parameter theories the addition of THF to PBI/DMAc dope solutions will favour delayed remixing and reduce the macrovoidal formation which is confirmed by SEM pictures (Figure 3.5).

Filtration experiments were performed in a cross-flow filtration apparatus and permeance (Figure 3.6) and rejection (Figure 3.7) were calculated according to Equation 1.2 and Equation 1.3 respectively.

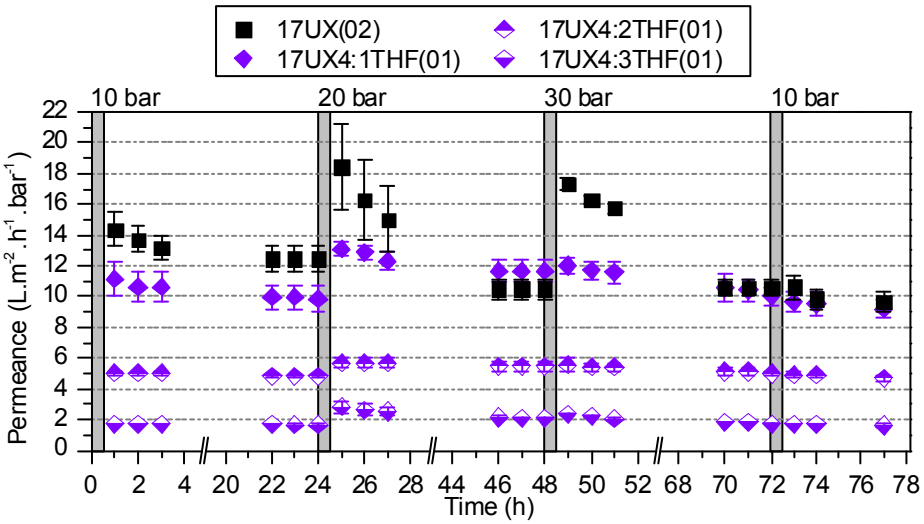

Figure 3.6 – Average PS/MeCN permeance, and standard deviation of uncrosslinked PBI membranes 17UX(02), 17UX4:1THF(01), 17UX4:2THF(01) and 17UX4:3THF(01) with 17 wt% polymer concentration and THF as a non-solvent in ratios 4:1, 4:2 and 4:3 respectively, at 30 °C with different pressures, for 77 hours

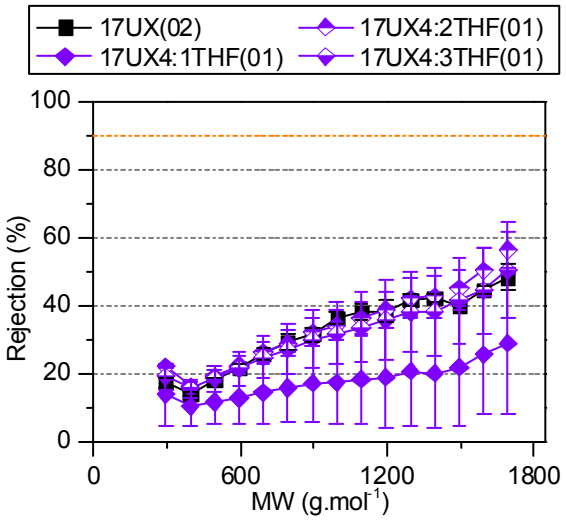

Figure 3.7 – Average PS rejection in MeCN, and standard deviation of uncrosslinked PBI membranes 17UX(02), 17UX4:1THF(01), 17UX4:2THF(01) and 17UX4:3THF(01) with 17 wt% polymer concentration and THF as a non-solvent in ratios 4:1, 4:2 and 4:3 respectively, at 30 ºC with different pressures, at 24, 48, 72 and 77 h

As it was observed in 3.1.2, permeance decreased in all membranes throughout the experiment, until it stabilised at the set pressure (Figure 3.6). This decrease was not so pronounced in the membranes with higher ratio of THF; 17UX4:2THF(01) and 17UX4:3THF(01). This is likely related to the lower presence of macrovoids in the structure of these two membranes (Figure 3.5). This low porosity leads to less free space for the polymer to rearrange.

Increasing the THF concentration in the dope solutions resulted in a decrease in permeance with the control membrane (from pure DMAc) having the highest permeance (Figure 3.6). It was possible to verify a trend between permeance and amount of THF added (Table 3.6). This might also be correlated with the parameters from Table 3.4 and Table 3.5. Since THF has a lower polarity index,

and higher partition coefficient than DMAc, delayed demixing occurred, leading to membranes with lower permeances.

However, the same was not true for PS rejections (Figure 3.7). SEM imaging and permeance results, supported by polarity index, partition coefficient and total solubility parameter, led to believe, that these membranes would have a MWCO within the NF range. This was not verified, and several hypotheses were considered. The polymer used by Livingston & Bhole, 2012 was synthesised in the laboratory, with a higher degree of purity and MW than the commercial one, which might have influenced the rejections.

Table 3.6 – Summary of the performance of PBI uncrosslinked membranes with different concentrations of THF in the dope solutions. Initial and final permeances and respective percentage decrease and the MWCO of the tested membranes

Membrane code	Permeance 1 hr, 10 bar ($L.m^{-2}.h^{-1}.bar^{-1}$)	Permeance 77 hr,10 bar ($L.m^{-2}.h^{-1}.bar^{-1}$)	Decrease (%)	MWCO ($g.mol^{-1}$)
17UX(02)	14.4	9.6	33	> 1 800
17UX4:1THF(01)	11.1	9.2	17	> 1 800
17UX4:2THF(01)	5.0	4.7	6	> 1 800
17UX4:3THF(01)	1.7	1.6	6	> 1 800

To overcome this, it was decided to proceed the experiments with crosslinked membranes, anticipating, more stable membranes and easier to reproduce.

4. Crosslinked membranes

4.1. Effect of crosslinking on membrane performance

4.1.1. Experimental

Before initiating the study of multi-component systems with crosslinked polybenzimidazole membranes, a comparison between uncrosslinked and crosslinked PBI membranes had to be performed. The experiments in this chapter were conducted for 24 hours, at 30 ºC and 30 bar.

Celazole® S26 was diluted with DMAc to obtain the 17 wt% polymer concentration dope solutions and membranes were prepared following the procedure in 2.1.2.

4.1.2. Results and discussion

FT-IR was performed on uncrosslinked and crosslinked PBI membranes (Figure 4.1). The obtained spectrum for uncrosslinked PBI is in accordance with the spectra published in literature (Musto, Karasz & MacKnight, 1993) The spectrum of crosslinked PBI showed two new peaks at 2 920 and 2 850 cm^{-1}. The C-H (terminal C of the crosslinker) and C-N (that connects the crosslinker with the polymer) bonds are responsible for these two peaks, confirming the polymer crosslinking.

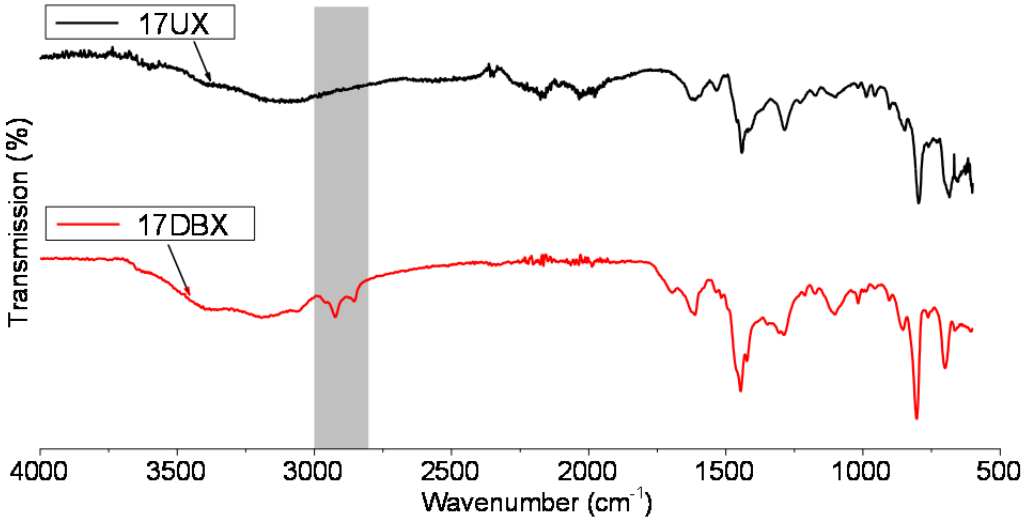

Figure 4.1 – FT-IR spectra for uncrosslinked and DBX crosslinked PBI membrane samples

SEM was carried out on the membranes to investigate the effect of chemical crosslinking on membrane morphology (Figure 4.2). The images show that more uniform tear-like pores were formed after crosslinking, and the membrane appeared to be thicker. The addition of the aromatic bi-functional crosslinker in the complex and the new connections formed between the polymer chains may contribute to pore stretching and a more uniform structure.

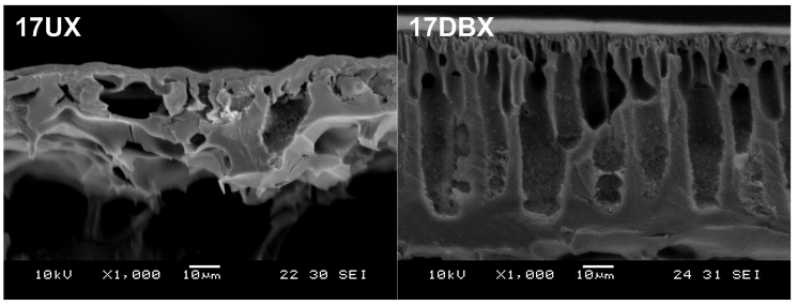

Figure 4.2 – SEM pictures of PBI uncrosslinked membrane 17UX and crosslinked 17DBX

Filtration was conducted during 24 hours at 30 ºC. Permeance and rejection (Figure 4.3) were calculated according to Equation 1.2 and Equation 1.3 respectively.

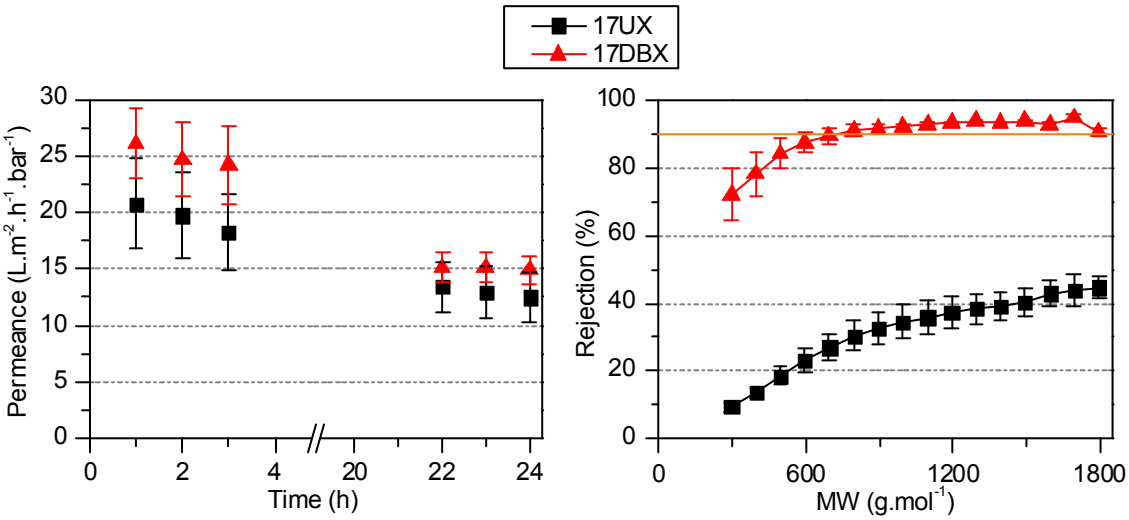

Figure 4.3 – Average PS/MeCN permeance and rejection of uncrosslinked and crosslinked PBI membranes with 17 wt% polymer concentration, at 30 °C and 30 bar, for 24 hours

After 24 hours of PS/MeCN filtration (Figure 4.3) the crosslinked membranes showed a rejection, in the NF range with a MWCO of 700 g.mol^{-1}, without the typical trade-off between rejection and permeance (Table 4.1). In fact, the permeance of crosslinked PBI was higher compared to the uncrosslinked membranes throughout the 24 hours filtration (Figure 4.3), which can be related to changes in the membrane structure upon crosslinking. The combination of these facts supported the idea that working with crosslinked membranes was the right path to follow. Throughout the experimental work, it was also possible to verify that the crosslinked membranes have better reproducibility.

Table 4.1 – Summary of PBI uncrosslinked and crosslinked membranes with 17 wt% polymer performance. Initial and final permeances and respective percentage decrease and the MWCO of the tested membranes

Membrane code	Permeance 1 hr, 30 bar ($L.m^{-2}.h^{-1}.bar^{-1}$)	Permeance 24 hr,30 bar ($L.m^{-2}.h^{-1}.bar^{-1}$)	Decrease (%)	MWCO ($g.mol^{-1}$)
17UX	20.8	12.5	40	> 1 800
17DBX	26.7	15.0	44	700

4.2. Multi-component systems

4.2.1. Experimental

Following the previous experiments, with addition of THF and the crosslinking of PBI membranes, it was time to start a study with a wider range of co/non-solvents. Solvents from different polarity groups were selected to find any relation between the chosen co/non-solvents and their impact on membrane performance. The total solubility parameter, $\Delta\delta_t$, with these solvent combinations was also calculated.

In total, seven co/non-solvents were tested. Three polar protic solvents – ethanol (EtOH), methanol (MeOH) and propan-2-ol (IPA); three polar aprotic solvents – *N,N*-dimethylformamide (DMF), acetonitrile (MeCN) and tetrahydrofuran (THF); and one non-polar solvent – 1,4-dioxane (DXN). The dope solutions were prepared with 17 wt% Celazole® S26 dissolved in DMAc and one of the above mentioned co/non-solvents in a ratio of 4:0.9 (DMAc:co/non-solvent). A ratio of 4:0.9 was chosen, because it was the highest amount of methanol possible to add, without precipitation of the polymer. Membranes were prepared following the procedure in 2.1.2.

Table 4.2 – Summary of prepared IS asymmetric PBI membranes and the physical characteristics of the dope solutions and casting conditions, for the multi-component systems study

Membrane Code	Co/Non-solvent	Water T (°C)	Room T (°C)	Room humidity (%)	Viscosity (cP)	Co/Non-solvent polarity
17DBX4:0.9EtOH(01)	EtOH	23	20	30	3 930	Polar Protic
17DBX4:0.9MeOH(01)	MeOH	23	20	40	3 450	
17DBX4:0.9MeOH(02)	MeOH	23	20	40	3 500	
17DBX4:0.9MeOH(03)	MeOH	23	20	30	3 450	
17DBX4:0.9IPA(01)	IPA	23	20	36	5 550	
17DBX4:0.9DMF(01)	DMF	23	20	38	5 680	Polar Aprotic
17DBX4:3DMF(01)	DMF	23	20	38	4 490	
17DBX4:3DMF(02)	DMF	23	20	40	20 080	
17DBX4:0.9MeCN(01)	MeCN	23	20	36	6 100	
17DBX4:0.9THF(01)	THF	23	20	34	14 760	
17DBX4:0.9DXN(01)	DXN	23	20	38	8 580	Non-Polar
17DBX4:3DXN(01)	DXN	23	20	40	11 470	
17DBX4:3DXN(02)	DXN	23	20	40	12 000	

4.2.2. Results and discussion

a) Addition of polar protic solvents

SEM was performed on the membranes to observe the effect of addition of polar protic solvents in the dope solution on membrane morphology (Figure 4.4).

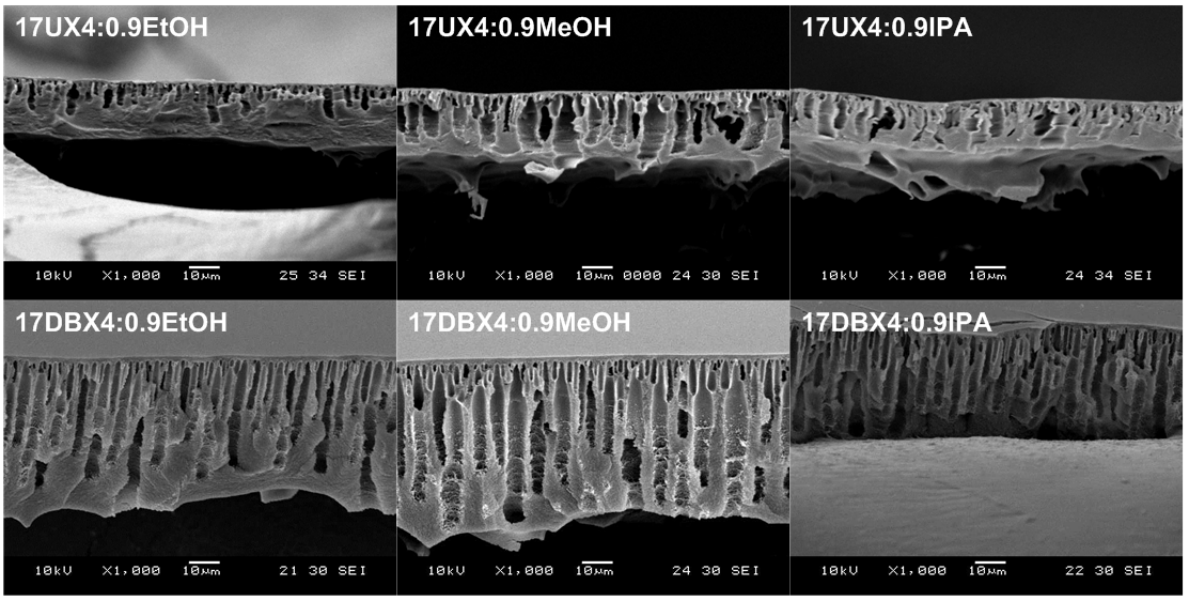

Figure 4.4 – SEM pictures of PBI uncrosslinked (top row) and crosslinked (bottom row) membranes with ethanol (EtOH), methanol (MeOH) and propan-2-ol (IPA) as Polar Protic non-solvents in a ratio of 4:0.9

Pictures showed that the addition of polar protic solvents had different impact on all membranes. The SEM picture of the membrane with EtOH as non-solvent would suggest that delayed demixing had occurred. When compared with the 17UX (Figure 4.2), 17UX4:0.9EtOH seems to have less macrovoids, and a sponge like structure (Figure 4.4). However, this is not supported by theory. The diffusivity coefficient, and polarity index (Table 4.3) of ethanol are quite high, and this would lead to instantaneous demixing. High diffusivity coefficient implies that ethanol would diffuse well in the water bath, and high polarity index means that ethanol would have good affinity with water.

SEM imaging of the 17UX4:0.9MeOH membrane (Figure 4.4) shows a membrane with long macrovoids. These macrovoids seem to be longer than the macrovoids from the 17UX (Figure 4.2) membrane and more uniform. These evidences lead to believe that instantaneous demixing occurred, as it was expected after calculating the diffusivity coefficient and partition coefficient and analysing the polarity index of methanol. Methanol has a high diffusivity coefficient, a negative partition coefficient and it is quite polar. All these factors imply good affinity and miscibility of methanol in water causing instantaneous demixing.

SEM analysis of 17UX4:0.9IPA membrane (Figure 4.4), allowed to observe a sponge like structure with some macrovoids. The membrane seems to be less porous than the 17UX membrane (Figure 4.2). Some delayed demixing is expected to have occurred. Of all the three polar protic solvents, IPA is the one with inferior diffusivity parameter, lower polarity index, and a positive partition coefficient (Table 4.3). Therefore delayed demixing was expected to take place.

Table 4.3 – Diffusivity parameter (Geankoplis, 1993; Poling, Prausnitz & O'Connell, 2001), Polarity index (Norman B. Godfrey, 1972) and partition coefficient (George Wypych, 2012) of EtOH, MeOH and IPA

Co/non-solvent	D_{AB} ($m^2.s^{-1}$)	Polarity Index (-)	Partition coefficient (-)	4:0.9 $\Delta\delta_t$ ($MPa^{1/2}$)
EtOH	1.407	5.2	-0.31	2.27
MeOH	1.795	5.1	-0.77	1.38
IPA	1.184	3.9	0.05	2.90

All these membranes seem to have undergone pore stretching after crosslinking (Figure 4.4). Membrane thickness also seems to have increased.

For comparison reasons, the uncrosslinked membranes were being taken in account, however, for performance, the crosslinked membranes were the evaluated ones.

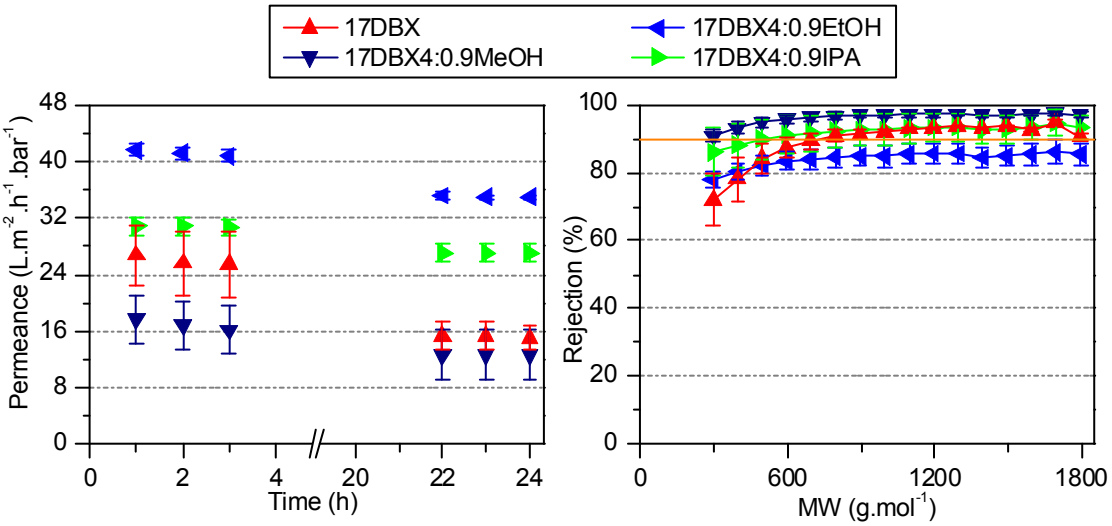

Figure 4.5 – Average PS/MeCN, permeance and rejection of the crosslinked PBI membranes with 17 wt% polymer and EtOH, MeOH and IPA as non-solvent in a ratio 4:0.9, at 30 °C and 30 bar after 24 hours

Regarding performance all membranes showed a good behaviour in the NF range (Figure 4.5). It was possible to obtain different MWCO and high permeances, similar or higher than the 17DBX membrane without co/non-solvent (Figure 4.5). When comparing the total solubility parameters (Table 4.3), it would be expected that the membrane with IPA would be the tightest membrane followed by the one with EtOH, and the MeOH membrane would be the more open membrane. However this was not the case. The IPA membrane had a MWCO of 500 $g.mol^{-1}$ but the EtOH one, had a MWCO > 1 800 $g.mol^{-1}$. And the membrane with MeOH ended up being the tightest membrane with a MWCO of 300 $g.mol^{-1}$. These results show that the total solubility parameter is not the only parameter to describe membrane formation and performance but the process is influenced by more parameters.

Nevertheless, these membranes seem to have good reproducibility. The 17DBX4:0.9MeOH curves in Figure 4.5 were obtained after preparing three membranes from three different dope solutions

prepared separately and the standard deviation of their permeance is around 3 $L.m^{-2}.h^{-1}.bar^{-1}$ and rejection around 1 %.

b) Addition of polar aprotic solvents

SEM was performed on the membranes to investigate the effect of the addition of polar aprotic solvents to the dope solution on membrane morphology (Figure 4.6).

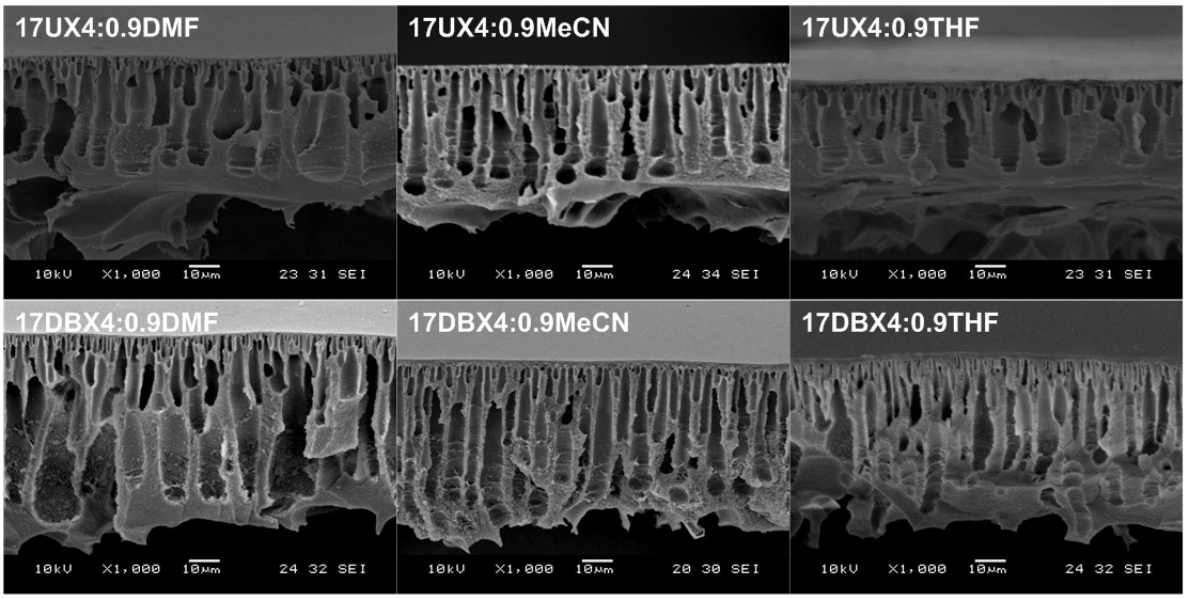

Figure 4.6 – SEM pictures of PBI uncrosslinked (top row) and crosslinked (bottom row) membranes with *N,N*-dimethylformamide (DMF), acetonitrile (MeCN) and tetrahydrofuran (THF) as Polar Aprotic co/non-solvents in a ratio of 4:0.9

Images from SEM showed once more, that every solvent had a different impact in membrane morphology when added as a co/non-solvent. Membrane 17UX4:0.9DMF (Figure 4.6) had large macrovoids in its structure suggesting that instantaneous had occurred. DMF has a high polarity index and negative partition coefficient (Table 4.4). These factors confirm the good affinity between DMF and water that lead to an instantaneous demixing during phase inversion.

The SEM picture of the membrane with addition of MeCN showed long tear-like pores (Figure 4.6). This membrane had a very uniform structure even before crosslinking. Instantaneous demixing was also expected from the addition of MeCN since it also has a high polarity index and a negative partition coefficient (Table 4.4) both imply a good miscibility with water, and therefore instantaneous demixing.

THF was once more tested as a non-solvent (3.2), but this time in a ratio of 4:0.9. The obtained membrane pore structure suggests delayed demixing had occurred was once more shown. A sponge-like structure with more macrovoids than in the previous study was obtained due to the lower concentration of THF (Figure 4.6). This effect is supported by the relatively lower polarity index and positive partition coefficient (Table 4.4) that suggest lower affinity between THF and water.

Table 4.4 – Diffusivity parameter (Geankoplis, 1993; Poling, Prausnitz & O'Connell, 2001), Polarity index (Norman B. Godfrey, 1972) and partition coefficient (George Wypych, 2012) of DMF, MeCN and THF

Co/non-solvent	D_{AB} ($m^2.s^{-1}$)	Polarity Index (-)	Partition coefficient (-)	4:0.9 $\Delta\delta_t$ ($MPa^{1/2}$)
DMF	-	6.4	-1.01	2.69
MeCN	-	5.8	-0.34	2.69
THF	1.184	4.0	0.46	4.13

Once more, crosslinking seemed to have cause pore elongation and thickening of the membrane structure (Figure 4.6).

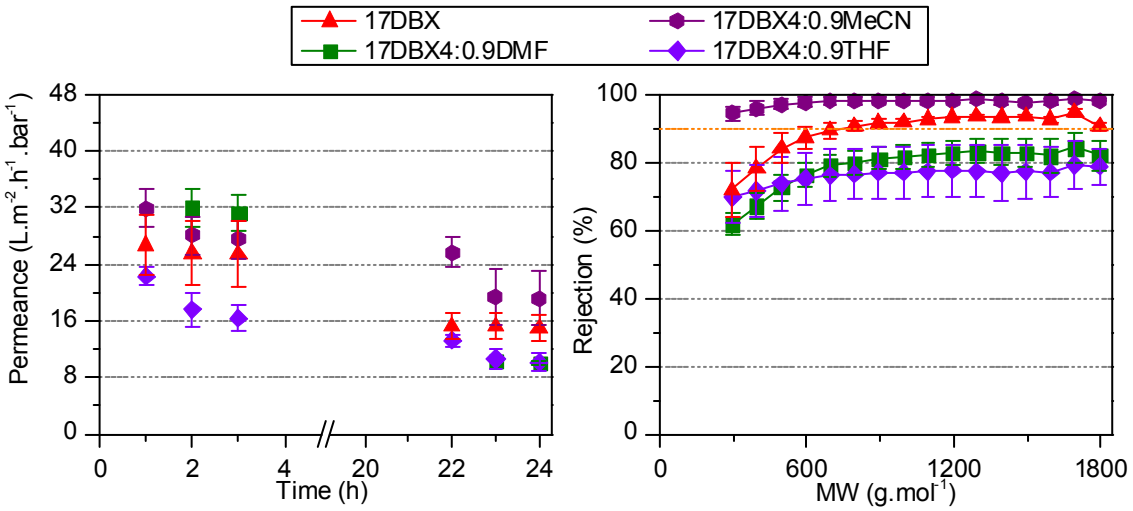

Figure 4.7 – Average PS/MeCN, permeance and rejection of the crosslinked PBI membranes with 17 wt% polymer and DMF, MeCN and THF as co/non-solvent in a ratio 4:0.9, at 30 °C and 30 bar after 24 hours

Addition of polar aprotic solvents seemed to have led to the formation of more opened membranes, meaning that they have a high MWCO outside the NF range (Figure 4.7). The membranes with DMF and THF had MWCO > 1 800 $g.mol^{-1}$. However the membrane with MeCN was the tightest one obtained in this project. The membrane had high permeance and MWCO < 200 $g.mol^{-1}$ (Figure 4.7). MeCN and DMF have the same total solubility parameter (Table 4.4); however, regarding rejection their behaviour was very different. THF had the highest total solubility parameter, and lowest rejection, contradicting once more the theory.

c) Addition of non-polar solvent

SEM was performed to investigate the effect of the addition of non-polar solvent on membrane morphology (Figure 4.8).

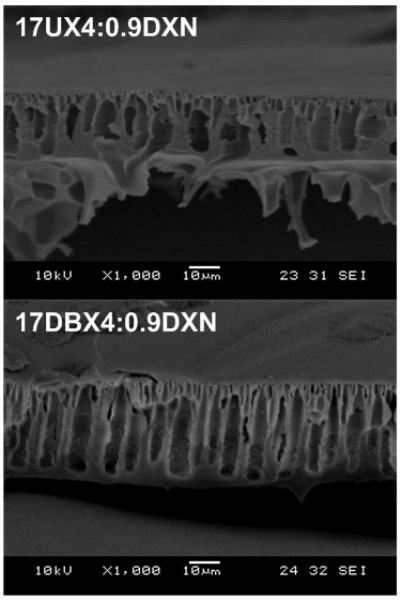

Figure 4.8 – SEM pictures of PBI uncrosslinked (top row) and crosslinked (bottom row) membranes with 1,4-dioxane (DXN) as Non-Polar non-solvent in a ratio of 4:0.9

SEM pictures of 17UX4:0.9DXN show a sponge-like structure with some macrovoids (Figure 4.8). Delayed demixing seems to have occurred. DXN has a low polarity index suggesting that its affinity with water is not as high as some solvents mentioned before (Table 4.5). The solvent has a negative partition coefficient, however, still close to zero. These parameters seem to support the fact that delayed demixing might have taken place.

Table 4.5 – Diffusivity parameter (Geankoplis, 1993; Poling, Prausnitz & O'Connell, 2001), Polarity index (Norman B. Godfrey, 1972) and partition coefficient (George Wypych, 2012) of DXN

Co/non-solvent	D_{AB} ($m^2.s^{-1}$)	Polarity Index (-)	Partition coefficient (-)	4:0.9 $\Delta\delta_t$ ($MPa^{1/2}$)
DXN	1.128	4.8	-0.27	3.61

Crosslinking the membrane caused the same effect in this membrane as in the previous ones, with a pore enlargement occurring.

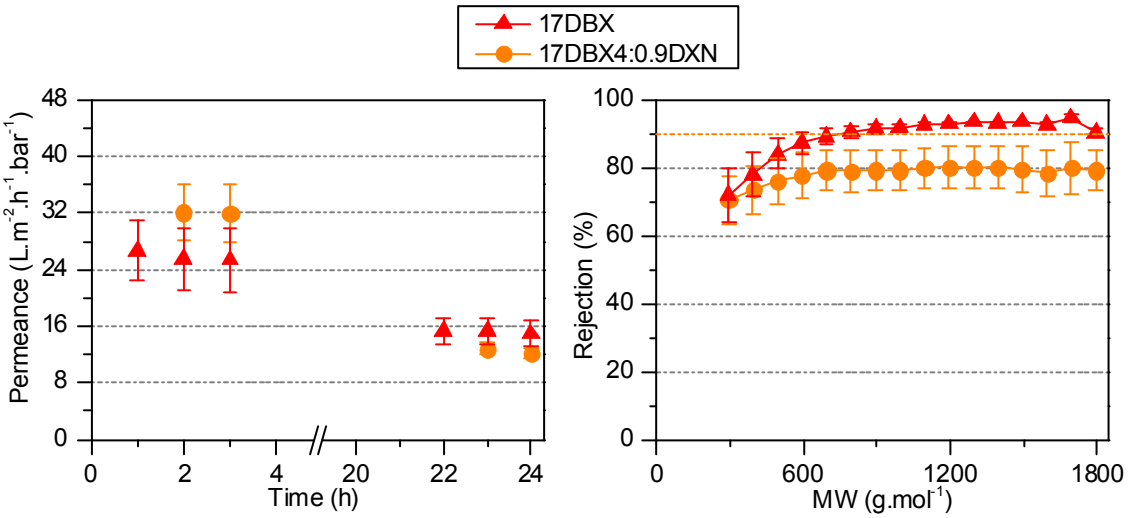

Figure 4.9 – Average PS/MeCN, permeance and rejection of the crosslinked PBI membranes with 17 wt% polymer and DXN as non-solvent in a ratio 4:0.9, at 30 °C and 30 bar after 24 hours

The 17DBX4:0.9DXN membrane had lower permeance, and a higher MWCO than the 17DBX (Figure 4.9). The delayed demixing and high total solubility parameter would suggest that this membrane would have a lower MWCO value than the control membrane, however this was not verified.

d) Effect of total solubility parameter with increasing addition of co/non-solvent

In order to compare the effect of the total solubility parameter on the same solvent but with different ratios, two solvents were chosen to be added as co/non-solvent in the dope solution – DMF and DXN.

Scanning Electron Microscopy was performed of the membranes to understand how the different ratios of co/non-solvent in the dope solution affect membrane morphology (Figure 4.10).

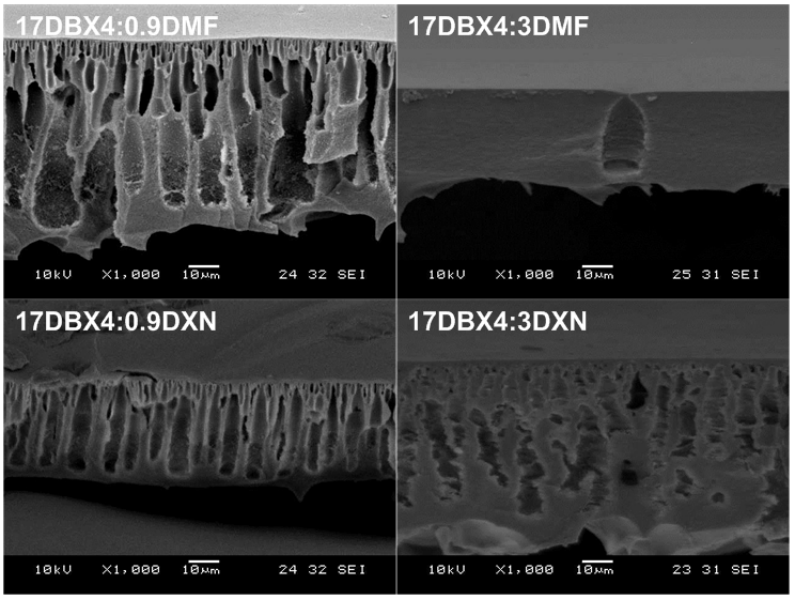

Figure 4.10 – SEM pictures of PBI crosslinked membranes with a ratio of 4:0.9 of DMF and DXN as co/non-solvent (on the left) and a ratio of 4:3 of DMF and DXN as co/non-solvent (on the right)

SEM showed that the addition of DMF and DXN in a ratio of 4:3, made the membranes tighter than the 17DBX (Figure 4.2), and tighter than the 17DBX4:0.9DMF and 17DBX4:0.9DXN (Figure 4.10). The addition of more DMF in dope solution decreases the total solubility parameter, while the addition of more DXN increases the solubility parameter (Table 4.6). The main goal was to investigate if the increment of the total solubility parameter with the same solvent would lead to the formation of a tighter membrane and the decrease of the total solubility parameter would lead to the formation of a looser membrane. This was only confirmed for the membranes prepared with different concentrations of DXN (Figure 4.11) as seen by Soroko et.al. In the case of increasing DMF concentration and decrease of solubility parameter the expected more open membrane was not obtained. In fact, the increased concentration resulted in a membrane tighter than the DXN prepared one (Figure 4.11). We can conclude that the total solubility parameter can be used, but it is not always accurate in predicting membrane performance and morphology structures.

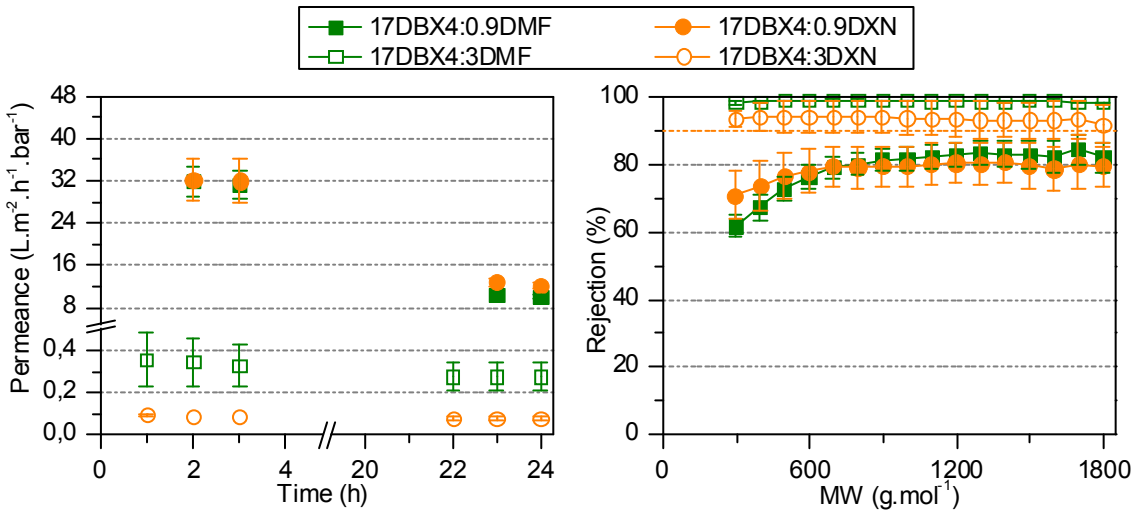

Figure 4.11 – Average PS/MeCN permeance and rejection of the crosslinked PBI membranes with 17 wt% polymer and DMF and DXN as co/non-solvent in a ratio of 4:0.9 and 4:3, at 30 °C and 30 bar after 24 hours

Permeance result and rejection were in accordance with membrane morphology (Figure 4.11). The membranes with a ratio of 4:3 of co/non-solvent had very low permeances and very high rejections as compared to membranes prepared with 4:0.9 ratios (Table 4.6).

Table 4.6 – Summary of PBI crosslinked membranes with 17 wt% polymer performance with DMF and DXN as co/non-solvents in the dope solution in different ratios. Initial and final permeances and respective percentage decrease, MWCO and total solubility parameter of the tested membranes

Membrane code	Permeance 1 hr, 30 bar ($L.m^{-2}.h^{-1}.bar^{-1}$)	Permeance 24 hr,30 bar ($L.m^{-2}.h^{-1}.bar^{-1}$)	Decrease (%)	MWCO ($g.mol^{-1}$)	$\Delta\delta_t$ ($MPa^{1/2}$)
17DBX4:0.9DMF	31.9	10.1	68	>1800	2.69
17DBX4:3DMF	0.4	0.3	25	< 200	1.92
17DBX4:0.9DXN	32.1	12.2	62	>1800	3.61
17DBX4:3DXN	0.1	0.1	0	< 200	4.10

4.3. Effect of post-treatment on MWCO and permeance of PBI membranes

4.3.1. Experimental

A work not directly related to the study of multi-component systems was also conducted during this dissertation. The purpose of this study was to investigate the impact of the conditioning agent on MWCO in PBI membranes. The reason for this is the hypothesis of controlled pore collapse due to evaporation of the volatile solvent, in our case IPA. In other words, a low concentration of PEG would lead to higher pore collapse due to lesser presence of non-volatile conditioner and vice versa, higher PEG concentration would prevent pore collapse and keep the pores open.

17 wt% polymer, crosslinked PBI membranes were prepared in accordance with 2.1.2 (Table 4.6), and impregnated in PEG_{400}/IPA solutions with different concentrations of PEG_{400} – 0, 5, 10, 25, 50, 75 and 100%. These membranes were tested in a cross-flow filtration apparatus for 24 hour, at 30 ºC and 30 bar.

Table 4.7 – Summary of prepared IS asymmetric PBI membranes and the physical characteristics of the dope solutions and casting conditions, for the post-treatment study

Membrane Code	Water T (°C)	Room T (°C)	Room humidity (%)	Viscosity (cP)	Post-treatment
17DBX0%PEG(01)	24	20	44	5 500	0%PEG
17DBX5%PEG(01)	24	20	44	5 500	5%PEG
17DBX10%PEG(01)	24	20	44	5 500	10%PEG
17DBX25%PEG(01)	24	20	46	5 450	25%PEG
17DBX25%PEG(02)	23	22	48	5 150	25%PEG
17DBX50%PEG(01)	24	20	46	5 450	50%PEG
17DBX50%PEG(02)	23	22	48	5 150	50%PEG
17DBX75%PEG(01)	24	20	46	5 450	75%PEG
17DBX75%PEG(02)	23	22	48	5 150	75%PEG
17DBX100%PEG(01)	24	20	46	5 450	100%PEG
17DBX100%PEG(02)	23	22	48	5 150	100%PEG

4.3.2. Results and discussion

To study membrane performance, a cross-flow filtration apparatus with eight cells filtration was used to conduct the experiments.

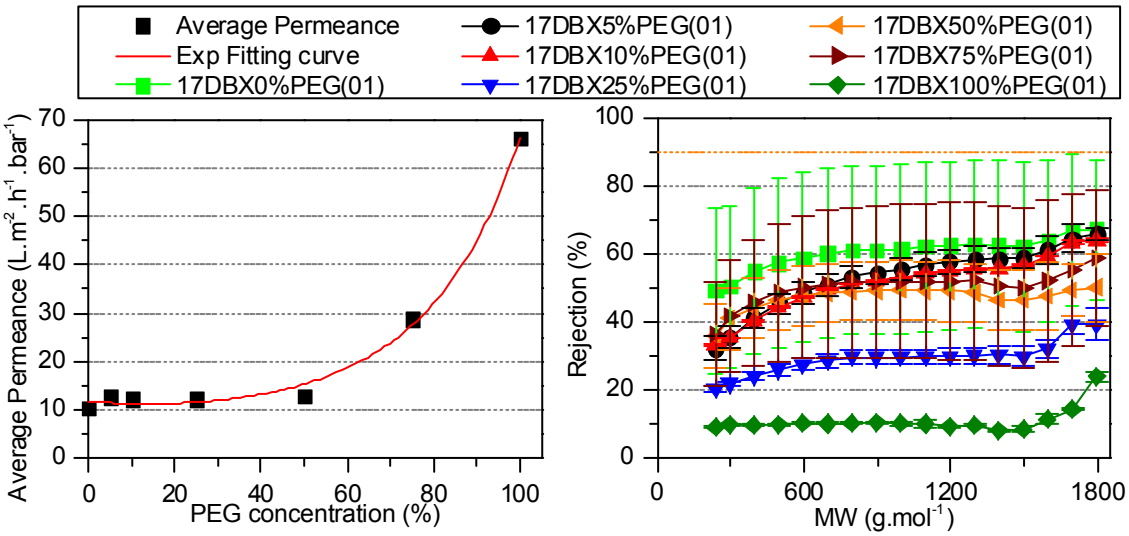

Figure 4.12 – Average permeance and rejection of the crosslinked PBI membranes with 17 wt% polymer impregnated in different PEG concentrations, with PS dissolved in MeCN, at 30 °C, 30 bar after 24 hours of experiment

In a first trial (Figure 4.12), after evaluating the permeances, it seemed that impregnating PBI membranes with different concentrations of PEG400 actually had an impact, and an exponential trend of the permeances was observed, possibly due to the fact that the membranes with more open pores were obtained with higher concentrations of PEG. Apart from this fact, the rejections did not follow a trend. Furthermore, the rejection of 17DBX50%PEG(01), which is the control membrane 17DBX, did not correspond to the regular rejection profile characteristic of 17 wt% polymer, crosslinked PBI membrane – compare Figure 4.3 and Figure 4.12. Therefore, there was a need to verify the accuracy of those results.

New membranes were prepared, from new dope solutions, and after a second trial (Figure 4.13), the exponential trend in permeances was not obtained as before. The concentration of PEG did not affect the rejection and permeances of the membranes, both parameters are overlapping in Figure 4.13. However, rejections were more in accordance with the regular rejection profile of 17 wt% polymer, crosslinked PBI membranes (control membrane).

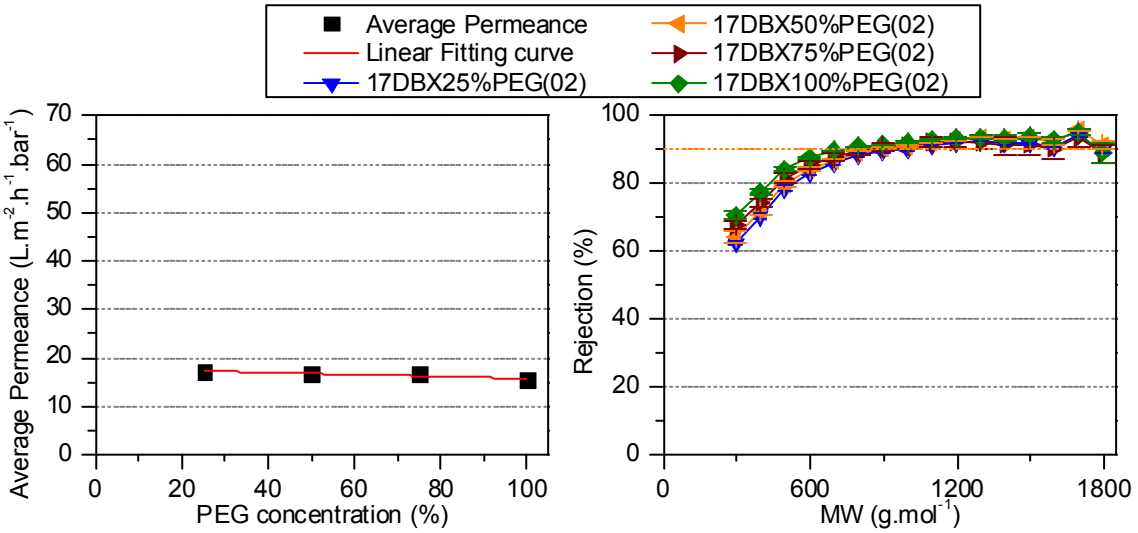

Figure 4.13 – Average permeance and rejection of the crosslinked PBI membranes with 17 wt% polymer impregnated in different PEG concentrations, with PS dissolved in MeCN, at 30 °C, 30 bar after 24 hours of reproducibility experiment

No conclusions can be taken so far from these experiments and more work needs to be conducted in order to have reliable data about the impact of this post-treatment in membrane performance. The hypothesis of controlled pore collapse using PEG could not be proven nor rejected.

5. Final conclusions and future work

In this work the formation of polybenzimidazole OSN membranes was demonstrated. In a first set of experiments it was confirmed that it is possible to control the MWCO of PBI uncrosslinked membranes just by changing the polymer concentration in the dope solution. Higher concentrations of polymer led to tighter membranes with lower MWCO and lower permeances. By increasing the pressure throughout these experiments, it was possible to observe the impact of pressure on membrane rejection. Higher pressures compacted the membrane and a lower MWCO was obtained. It was also possible to verify that this compaction is irreversible. After decreasing the pressure, the rejection profile remained the same.

In the second study, THF was added to the PBI dope solutions as a non-solvent in different ratios. Several parameters were considered to explain the structures and performances of the obtained membranes. The low polarity index and partition coefficient of THF suggested the formation of tighter membranes as the concentration of THF increased. This was confirmed for the morphology and the permeance, but not for the rejection. Due to the instability of uncrosslinked membranes no solid conclusions were taken, and there was a need to follow a different path in the experimental procedure.

The required membrane chemical and physical stability to proceed with the experiments was achieved through chemical crosslinking of PBI. The addition of several co/non-solvents in the same ratio led to the formation of PBI membranes with different MWCO in the NF range. Apart from good rejection profiles, these membranes showed high permeances, similar and some (17DBX4:0.9MeCN) higher than the crosslinked membranes without the addition of a co/non-solvent.

In order to have a better understanding of the impact of co/non-solvent addition of on membrane morphology and performance, a correlation between the experimental results and several solvent parameters was undertaken. However no relation was found between the total solubility parameters, partition coefficients, diffusivity parameter or polarity of the co/non-solvents and the performance of the membrane. A combination of all these factors must have an impact in membrane formation and consequently in membrane performance. More studies need to be conducted to achieve a deeper understanding of the influence of co/non-solvents in the dope solutions.

In a final stage, a post-treatment study was performed. Studies regarding the influence of controlled pore collapse with different concentrations of conditioning agent on membrane performance were not conclusive, and more experiments must be conducted to confirm or reject the hypothesis.

To conclude, different MWCOs were and can be achieved through polymer concentration variation and with the addition of different co/non-solvents in different ratios in the dope solutions. An attempt to correlate the functional membrane performance with different solvent properties was undertaken. Polarity index, diffusivity coefficient, partition coefficient and solubility parameters were calculated and analysed. However, no clear correlation could be obtained which would explain and predict membrane performance. More studies need to be conducted in order to have a better understanding, on a

fundamental level of the impact of these factors in PBI membrane formation and performance. From this dissertation, we know what affects membrane formation, however not the how and why, and these questions must still be answered.

6. References

Baker, R. (2004) *Membrane Technology and Applications*. 2nd Edition. Wiley.

Barton, A.F.M. (1983) *CRC handbook of solubility parameters and other cohesion parameters*. CRC Press.

Billmeyer, F.W. (1984) *Textbook of polymer science*. 3rd Edition. Wiley.

Bishop, M.T., Chau, C.-C., Koo, J., Racchini, J.R., *et al.* (1991) *Microporous peek membranes and the preparation thereof*.

Brandrup, J., Immergut, E.H. & Grulke, E.A. (2004) *Polymer handbook*. 4 th Edition. New York; Chichester, Wiley.

Van der Bruggen, B., Mänttäri, M. & Nyström, M. (2008) Drawbacks of applying nanofiltration and how to avoid them: A review. *Separation and Purification Technology*. [Online] 63 (2), 251–263. Available from: doi:10.1016/j.seppur.2008.05.010 [Accessed: 9 August 2013].

Chung, T.-S. (1997) A Critical Review of Polybenzimidazoles. *Journal of Macromolecular Science, Part C: Polymer Reviews*. [Online] 37 (2), 277–301. Available from: doi:10.1080/15321799708018367 [Accessed: 13 September 2013].

Cuperus, F.P. & Smolders, C.A. (1991) Characterization of UF membranes: Membrane characteristics and characterization techniques. *Advances in Colloid and Interface Science*. [Online] 34135–173. Available from: doi:10.1016/0001-8686(91)80049-P [Accessed: 20 August 2013].

Drioli, E. & Giorno, L. (2009) *Membrane Operations: Innovative Separations and Transformations*. Wiley.

Evonik MET Ltd. (n.d.) *Membrane Properties - DuraMem® and PuraMem®*. [Online]. Available from: http://duramem.evonik.com/product/duramem-puramem/en/about/membrane-properties/pages/default.aspx [Accessed: 9 August 2013].

Ferreira, F.C., Macedo, H., Cocchini, U. & Livingston, A.G. (2006) Development of a Liquid-Phase Process for Recycling Resolving Agents within Diastereomeric Resolutions. *Organic Process Research & Development*. [Online] 10 (4), 784–793. Available from: doi:10.1021/op0600456 [Accessed: 10 September 2013].

Geankoplis, C.J. (1993) *Transport processes and unit operations*. 3rd Edition. Engelwood Cliffs, N.J., PTR Prentice Hall.

Gedde, U.W. (1995) *Polymer Physics*. 1st Edition. Springer.

George Wypych (2012) Knovel Solvents A Properties Database. *ChemTech Publishing*.

Gibbins, E., D' Antonio, M., Nair, D., White, L.S., *et al.* (2002) Observations on solvent flux and solute rejection across solvent resistant nanofiltration membranes. *Desalination*. [Online] 147 (1–3), 307–313. Available from: doi:10.1016/S0011-9164(02)00557-X [Accessed: 9 August 2013].

Van der Gryp, P., Barnard, A., Cronje, J.-P., de Vlieger, D., *et al.* (2010) Separation of different metathesis Grubbs-type catalysts using organic solvent nanofiltration. *Journal of Membrane Science*. [Online] 353 (1–2), 70–77. Available from: doi:10.1016/j.memsci.2010.02.032 [Accessed: 10 September 2013].

Hendrix, K., Van Eynde, M., Koeckelberghs, G. & Vankelecom, I.F.J. (2013) Crosslinking of modified poly(ether ether ketone) membranes for use in solvent resistant nanofiltration. *Journal of*

Membrane Science. [Online] 447212–221. Available from: doi:10.1016/j.memsci.2013.07.002 [Accessed: 18 September 2013].

Jung, B., Yoon, J.K., Kim, B. & Rhee, H.-W. (2004) Effect of molecular weight of polymeric additives on formation, permeation properties and hypochlorite treatment of asymmetric polyacrylonitrile membranes. *Journal of Membrane Science*. [Online] 243 (1–2), 45–57. Available from: doi:10.1016/j.memsci.2004.06.011 [Accessed: 10 September 2013].

Kim, J.F., Freitas da Silva, A.M., Valtcheva, I.B. & Livingston, A.G. (2013) When the membrane is not enough: A simplified membrane cascade using Organic Solvent Nanofiltration (OSN). *Separation and Purification Technology*. [Online] 116277–286. Available from: doi:10.1016/j.seppur.2013.05.050 [Accessed: 9 August 2013].

Kumbharkar, S.C., Karadkar, P.B. & Kharul, U.K. (2006) Enhancement of gas permeation properties of polybenzimidazoles by systematic structure architecture. *Journal of Membrane Science*. [Online] 286 (1–2), 161–169. Available from: doi:10.1016/j.memsci.2006.09.030 [Accessed: 9 August 2013].

Leo, A., Hansch, C. & Elkins, D. (1971) Partition coefficients and their uses. *Chemical Reviews*. [Online] 71 (6), 525–616. Available from: doi:10.1021/cr60274a001 [Accessed: 18 September 2013].

Li, Q., He, R., Jensen, J. o. & Bjerrum, N. j. (2004) PBI-Based Polymer Membranes for High Temperature Fuel Cells – Preparation, Characterization and Fuel Cell Demonstration. *Fuel Cells*. [Online] 4 (3), 147–159. Available from: doi:10.1002/fuce.200400020 [Accessed: 9 August 2013].

Livingston, A.G. & Bhole, Y.S. (2013) *Asymmetric membranes for use in nanofiltration*.

Livingston, A.G. & Bhole, Y.S. (2012) *Asymmetric Membranes for Use in Nanofiltration*. [Online]. Available from: http://patentscope.wipo.int/search/en/detail.jsf?docId=WO2012010886&recNum=32&tab=Drawings&maxRec=2733&office=&prevFilter=&sortOption=&queryString=%28benzimidazol*+AND+%28pyrid*+AND+sulfin*+AND+sulfon*%29%29+ [Accessed: 29 August 2013].

Loeb, S. & Sourirajan, S. (1963) Sea Water Demineralization by Means of an Osmotic Membrane. In: *Saline Water Conversion—II*. [Online]. WASHINGTON, D. C., AMERICAN CHEMICAL SOCIETY. pp. 117–132. Available from: http://pubs.acs.org/doi/pdf/10.1021/ba-1963-0038.ch009 [Accessed: 11 September 2013].

Mulder, M. (1996) *Basic Principles of Membrane Technology*. Springer.

Musto, P., Karasz, F.E. & MacKnight, W.J. (1993) Fourier transform infra-red spectroscopy on the thermo-oxidative degradation of polybenzimidazole and of a polybenzimidazole/polyetherimide blend. *Polymer*. [Online] 34 (14), 2934–2945. Available from: doi:10.1016/0032-3861(93)90618-K [Accessed: 18 September 2013].

Norman B. Godfrey (1972) Solvent selection via miscibility number. *Chemtech*. 359–363.

Pinnau, I. & Freeman, B.D. (2000) *Membrane formation and modification*. American Chemical Society.

Poling, B.E., Prausnitz, J.M. & O'Connell, J.P. (2001) *The properties of gases and liquids*. 5thEdition edition. New York, McGraw-Hill.

Porter, M.C. (1990) *Handbook of Industrial Membrane Technology*. Noyes Publications.

Reddy, K.K., Kawakatsu, T., Snape, J.B. & Nakajima, M. (1996) Membrane Concentration and Separation of L-Aspartic Acid and L-Phenylalanine Derivatives in Organic Solvents. *Separation Science and Technology*. [Online] 31 (8), 1161–1178. Available from: doi:10.1080/01496399608001340 [Accessed: 10 September 2013].

Richard Bowen, W. & Doneva, T.A. (2000) Atomic force microscopy studies of nanofiltration membranes: surface morphology, pore size distribution and adhesion. *Desalination*. [Online] 129 (2), 163–172. Available from: doi:10.1016/S0011-9164(00)00058-8 [Accessed: 9 August 2013].

Rundquist, E., Pink, C., Vilminot, E. & Livingston, A. (2012) Facilitating the use of counter-current chromatography in pharmaceutical purification through use of organic solvent nanofiltration. *Journal of Chromatography A*. [Online] 1229156–163. Available from: doi:10.1016/j.chroma.2012.01.021 [Accessed: 10 September 2013].

Sawyer, L.C. & Jones, R.S. (1984) Observations on the structure of first generation polybenzimidazole reverse osmosis membranes. *Journal of Membrane Science*. [Online] 20 (2), 147–166. Available from: doi:10.1016/S0376-7388(00)81329-0 [Accessed: 9 August 2013].

See Toh, Y.H., Lim, F.W. & Livingston, A.G. (2007) Polymeric membranes for nanofiltration in polar aprotic solvents. *Journal of Membrane Science*. [Online] 301 (1–2), 3–10. Available from: doi:10.1016/j.memsci.2007.06.034 [Accessed: 9 August 2013].

See Toh, Y.H., Loh, X.X., Li, K., Bismarck, A., *et al.* (2007) In search of a standard method for the characterisation of organic solvent nanofiltration membranes. *Journal of Membrane Science*. [Online] 291 (1–2), 120–125. Available from: doi:10.1016/j.memsci.2006.12.053 [Accessed: 20 August 2013].

See-Toh, Y.H., Ferreira, F.C. & Livingston, A.G. (2007) The influence of membrane formation parameters on the functional performance of organic solvent nanofiltration membranes. *Journal of Membrane Science*. [Online] 299 (1–2), 236–250. Available from: doi:10.1016/j.memsci.2007.04.047 [Accessed: 9 August 2013].

See-Toh, Y.H., Silva, M. & Livingston, A. (2008) Controlling molecular weight cut-off curves for highly solvent stable organic solvent nanofiltration (OSN) membranes. *Journal of Membrane Science*. [Online] 324 (1–2), 220–232. Available from: doi:10.1016/j.memsci.2008.07.023 [Accessed: 9 August 2013].

Sheth, J.P., Qin, Y., Sirkar, K.K. & Baltzis, B.C. (2003) Nanofiltration-based diafiltration process for solvent exchange in pharmaceutical manufacturing. *Journal of Membrane Science*. [Online] 211 (2), 251–261. Available from: doi:10.1016/S0376-7388(02)00423-4 [Accessed: 10 September 2013].

SolSep BV - Robust Membrane Technologies (n.d.) *Solsep membranes modules for organic membrane filtration separation*. [Online]. Available from: http://www.solsep.com/ [Accessed: 9 August 2013].

Soroko, I., Lopes, M.P. & Livingston, A. (2011) The effect of membrane formation parameters on performance of polyimide membranes for organic solvent nanofiltration (OSN): Part A. Effect of polymer/solvent/non-solvent system choice. *Journal of Membrane Science*. [Online] 381 (1–2), 152–162. Available from: doi:10.1016/j.memsci.2011.07.027 [Accessed: 30 August 2013].

Soroko, I., Makowski, M., Spill, F. & Livingston, A. (2011) The effect of membrane formation parameters on performance of polyimide membranes for organic solvent nanofiltration (OSN). Part B: Analysis of evaporation step and the role of a co-solvent. *Journal of Membrane Science*. [Online] 381 (1–2), 163–171. Available from: doi:10.1016/j.memsci.2011.07.028 [Accessed: 30 August 2013].

Strathmann, H. & Kock, K. (1977) The formation mechanism of phase inversion membranes. *Desalination*. [Online] 21 (3), 241–255. Available from: doi:10.1016/S0011-9164(00)88244-2 [Accessed: 12 September 2013].

Székely, G., Bandarra, J., Heggie, W., Sellergren, B., *et al.* (2012) A hybrid approach to reach stringent low genotoxic impurity contents in active pharmaceutical ingredients: Combining molecularly imprinted polymers and organic solvent nanofiltration for removal of 1,3-

diisopropylurea. *Separation and Purification Technology*. [Online] 8679–87. Available from: doi:10.1016/j.seppur.2011.10.023 [Accessed: 10 September 2013].

U. Razdan, S.V. Joshi & V. J. Shah (2003) Novel membrane processes for separation of organics. *Current Science India*. 85 (06), 761–771.

Valadez-Blanco, R., Ferreira, F.C., Jorge, R.F. & Livingston, A.G. (2008) A membrane bioreactor for biotransformations of hydrophobic molecules using organic solvent nanofiltration (OSN) membranes. *Journal of Membrane Science*. [Online] 317 (1–2), 50–64. Available from: doi:10.1016/j.memsci.2007.04.032 [Accessed: 10 September 2013].

Vandezande, P., Gevers, L.E.M. & Vankelecom, I.F.J. (2008) Solvent resistant nanofiltration: separating on a molecular level. *Chemical Society Reviews*. [Online] 37 (2), 365–405. Available from: doi:10.1039/B610848M [Accessed: 9 August 2013].

Vandezande, P., Li, X., Gevers, L.E.M. & Vankelecom, I.F.J. (2009) High throughput study of phase inversion parameters for polyimide-based SRNF membranes. *Journal of Membrane Science*. [Online] 330 (1–2), 307–318. Available from: doi:10.1016/j.memsci.2008.12.068 [Accessed: 12 September 2013].

Wang, K.Y., Xiao, Y. & Chung, T.-S. (2006) Chemically modified polybenzimidazole nanofiltration membrane for the separation of electrolytes and cephalexin. *Chemical Engineering Science*. [Online] 61 (17), 5807–5817. Available from: doi:10.1016/j.ces.2006.04.031 [Accessed: 9 August 2013].

White, L.S. (2006) Development of large-scale applications in organic solvent nanofiltration and pervaporation for chemical and refining processes. *Journal of Membrane Science*. [Online] 286 (1–2), 26–35. Available from: doi:10.1016/j.memsci.2006.09.006 [Accessed: 10 September 2013].

Wu, Q.-Y., Wan, L.-S. & Xu, Z.-K. (2012) Structure and performance of polyacrylonitrile membranes prepared via thermally induced phase separation. *Journal of Membrane Science*. [Online] 409–410355–364. Available from: doi:10.1016/j.memsci.2012.04.006 [Accessed: 9 August 2013].

Zhao, Z.-P., Li, J., Wang, D. & Chen, C.-X. (2005) Nanofiltration membrane prepared from polyacrylonitrile ultrafiltration membrane by low-temperature plasma: 4. grafting of N-vinylpyrrolidone in aqueous solution. *Desalination*. [Online] 184 (1–3), 37–44. Available from: doi:10.1016/j.desal.2005.04.036 [Accessed: 9 August 2013].